EXAMINING THE ROLES OF β-CATENIN AND HDAC6 IN PRIMARY CILIA SIGNALING IN ccRCC AND CRC

A Thesis

by

ASHLEY L PERKINS

Submitted to the Office of Graduate and Professional Studies of
Texas A&M University
in partial fulfillment of the requirement for the degree of

MASTER OF SCIENCE

Chair of Committee,	Cheryl L. Walker
Co-chair of Committee,	Roderick H. Dashwood
Committee Member,	Peter Davies

August 2015

Major Subject: Medical Sciences

ABSTRACT

Primary cilia are single hair-like organelles found on the apical surface of growth arrested and differentiated cells and can be found in almost every cell type, including epithelial cells, fibroblasts, olfactory neurons and photoreceptors, which reflect their diverse cellular functions. The primary cilium forms upon entry into G_0; preceding G_0 arrest, the cilium resorbs through mechanisms involving deacetylation of the tubulin by specific deacetylases. Functionally, the primary cilium acts as a mechanosenor, chemosensor and osmosensor for the cell, detecting its neighboring cells and responding to extracellular signals. Due to its versatility in functions, dysregulation of the primary cilia has been associated with multiple human diseases and syndromes termed "ciliopathies", which include polycystic kidney and liver disease, primary ciliary dyskinesia, nephronophthisis and more recently, colon cancer.

Another primary cilia-related disorder is von Hippel-Lindau (VHL) disease is a systemic disorder predisposing patients to hemangioblastomas, phaeochromocytoma, and cysts in the kidney and pancreas. The loss of the VHL protein (pVHL) is the most common genetic mutation associated with clear cell renal cell carcinoma (ccRCC). Functionally, pVHL is an E3 ligase involved in targeting proteins, such as hypoxia inducible factor (HIF), epidermal growth factor (EGFR) and protein kinase Cγ (PKCγ) for proteasomal degradation and has been shown to be involved in microtubule stability and maintenance of the primary cilium; loss of pVHL is associated with loss of primary cilia. The mechanism by which pVHL regulates formation and function of the primary

cilium is not fully understood but is of importance, especially in the setting of renal cell carcinoma (RCC).

Recent studies indicate that Aurora kinase-A (AURKA), a mitotic kinase, plays an important role in the resorption of primary cilia via interaction of human enhancer of filamentation 1 (HEF1) and activation of histone deacetylase 6 (HDAC6). Our studies show that in the absence of pVHL, AURKA is upregulated, leading to activation of HDAC6, shortening the primary cilia. Given that pVHL stabilizes Jade-1 to promote degradation of β-catenin, we investigated the role of β-catenin in transcriptionally maintaining AURKA levels. We found that in VHL-null cells, activated β-catenin translocates to the nucleus, increasing AURKA mRNA and protein levels. Using an inhibitor of β-catenin driven-transcription, iCRT14, we were able to rescue aberrant AURKA signaling and the ciliary defect in VHL deficient cells. Thus, our studies have identified a pathway that regulates primary cilia in the setting of RCC with two potential targets, for therapeutic intervention. Additionally, direct roles for primary cilia in colon tumorigenesis have yet to be studied in depth. The adenomatous polyposis coli (APC)/β-catenin Wnt signaling proteins, commonly dysregulated in colon cancer, have independently been localized to microtubules and are transported along the structures, via KIF3α. Additional evidence supports β-catenin being a crucial facilitator of ciliopathies. Here, we present evidence for a role of primary cilia in colon cancer, demonstrating how dysregulation of Wnt pathway proteins correlates with loss of primary cilia. Our data also provide support for similarities between the colon and kidney with regards to ciliary maintenance and the mechanisms involved.

DEDICATION

To my family for all of their love, support and guidance.

ACKNOWLEDGEMENTS

I would like to thank my committee members Dr. Cheryl Walker, Dr. Roderick Dashwood and Dr. Peter Davies for all of their expertise throughout the course of this research. I appreciate all of the time taken to discuss my research projects and advise me when necessary. I would like to acknowledge everyone in the Walker and Dashwood labs for their support and advice throughout my graduate career. Thanks also go to the friends and colleagues I have met along with way in the departments of Translational Cancer Research and Center for Epigenetics and Disease Prevention for making my time at the IBT an experience I will never forget. I appreciate all of the assistance and useful talks that have directed me toward my goals.

Thanks to my friends, both near and far, for their constant optimism, always making me laugh and allowing me to be a part of the special moments and milestones in their lives. A special thanks to my mentor, Brad Bryan for pushing me in the right direction. Your advice never goes unheard. Thanks to all of my family for their encouraged support and guidance over the past twenty six years, especially my mother; your unconditional love and dedication have pushed me further than you could ever imagine. All of the qualities that people love about me I get from you. To my boyfriend and best friend Reid, thank you for your love, support and most of all patience over the past three years. You have kept me sane.

TABLE OF CONTENTS

Page

LIST OF FIGURES

Page

CHAPTER I

INTRODUCTION TO PRIMARY CILIA

BACKGROUND

Primary cilia are single hair-like organelles found on the apical surface of growth arrested and differentiated cells [1-3]. Almost all vertebrate cells contain primary cilia which are sheathed by a ciliary membrane that covers the ciliary axoneme, consisting of nine microtubule doublets made up of α-tubulin/ β-tubulin dimers [4, 5, 6]. Cilia can be separated into two categories: motile cilia and primary cilia. Motile cilia contain a pair of microtubule singlets found in the center of the axoneme giving it a 9+2 confirmation, differentiating it from the primary cilium which lacks this central pair, giving it a 9+0 arrangement (Figure 1) [7, 8]. Therefore, the functions of primary cilia differ from that of motile cilia. Cells, such as those in the trachea, can house multiple motile cilia whose function is to move in wave-like patterns to push fluid through [9]. Motile cilia produce this synchronous beating pattern through interactions between the dynein arms and microtubules [9]. Primary cilia, on the other hand, lack this movement and function as antennas for the cell, receiving extracellular signals, transmitting them down the axoneme via intraflagellar transport (IFT). Therefore, primary cilia are often found in the lumen of organs such as the aorta, kidney, and colon (Figure 2) [10-12]. The axoneme is anchored to the cell by a basal body made up of the mother centriole [13] (Figure 1). Due to the mother centriole's dual role in ciliogenesis and cell division, disassembly of

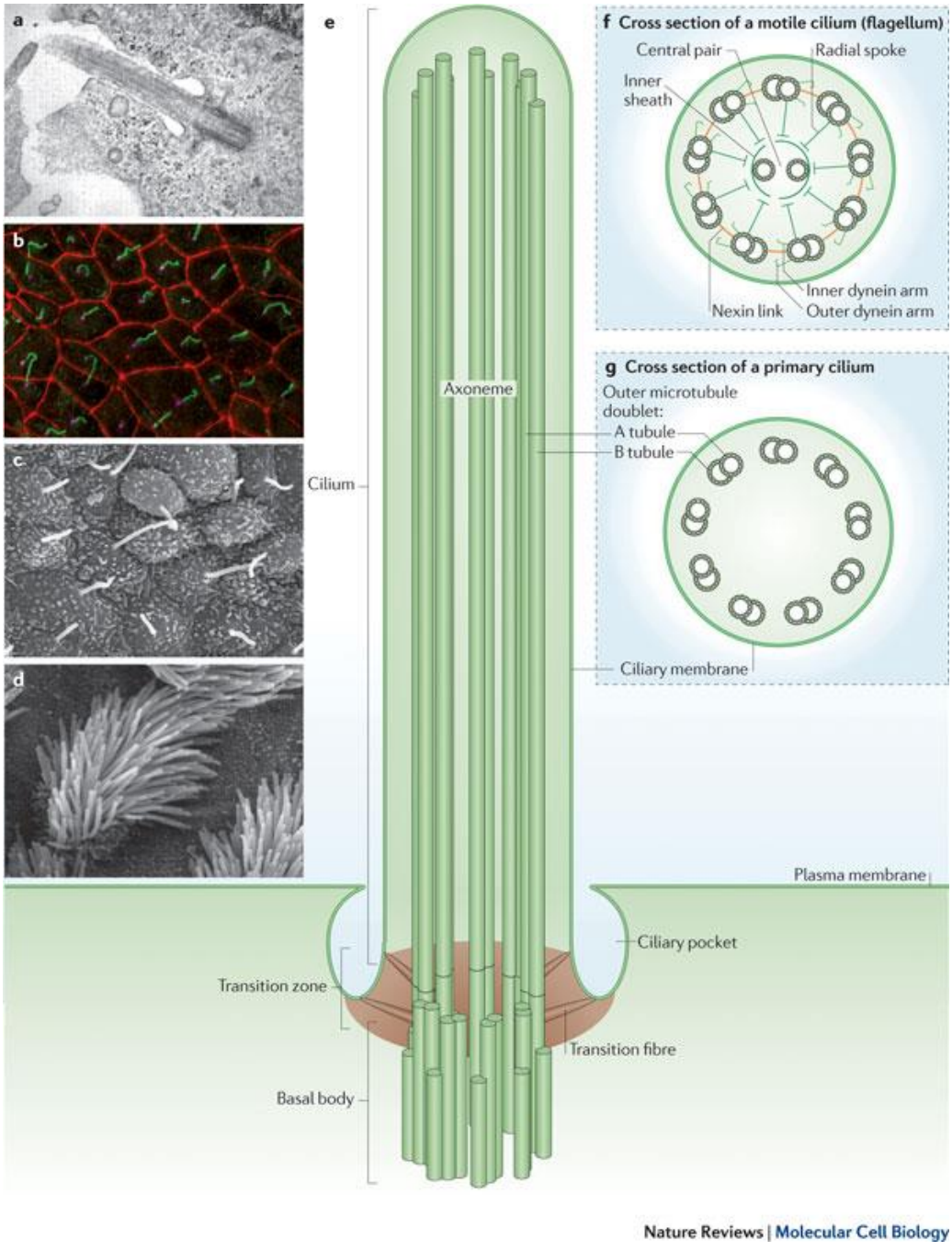

Figure 1. A simplified version of ciliary architecture. (A-D) hTERT RPE1cells, IMCD3 cells, mouse nodal and mouse tracheal cells are shown containing cilia, respectively. (E) The basic structure of the cilium is shown next to (F) cross section schematics of motile and (G) primary cilia.

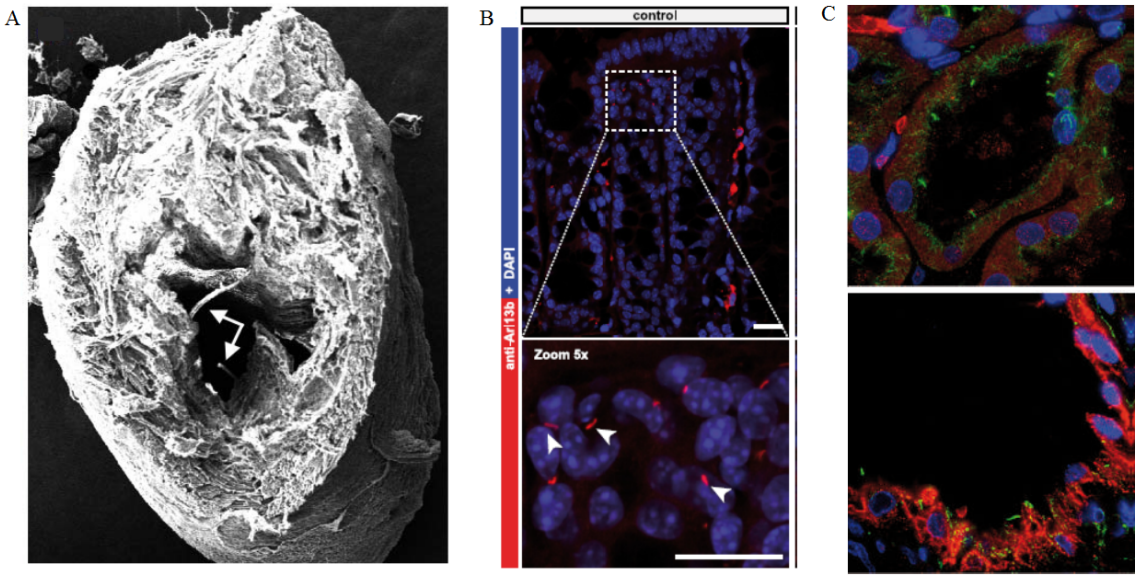

Figure 2. Primary cilia in the lumen. (A) EM of primary cilia in the lumen of embryonic aorta [11]. (B) Confirmation of the presence of primary cilia in colon crypts [10]. (C) Primary cilia staining in the renal tubule of normal (top) and cancerous tissue (bottom).

the primary cilium is a prerequisite for proliferation, therefore they are mutually exclusive events [3].

CILIA-CENTROSOME CYCLE

During mitosis, the centrioles function in spindle formation. Once, mitosis is complete, the centrioles then migrate toward the plasma membrane where the axoneme begins to grow from the mother centriole, now called the basal body, followed by elongation of the primary cilium [3]. The primary cilium forms during G_0/G_1 and usually resorbs by the time the cell reaches mitosis [3]. Formation in cell culture is dependent on cell confluence and lack of growth factors, therefore the simplest way to get cells to ciliate in cell culture is by serum starvation once they have reached confluency as shown by Pugacheva et al. 2007 [14]. Pugacheva also demonstrated a role for aurora kinase A (AURKA), a mitotic regulator found at the centrosome, localizing the protein to the

basal body where it interacts with human elongation factor 1 (HEF1), subsequently activating histone deacetylase 6 (HDAC6) [14]. HDAC6 functions to deacetylate α-tubulin, causing depolymerization and resorption of the cilium [14]. Throughout recent years, more proteins have been found to play a role in the relationship between cilia and the cell cycle [15]. When the cell is signaled to divide again, through various mechanisms, the primary cilium resorbs and shortens until the mother centriole is released and is recycled for another round of division [3, 16] (Figure 3).

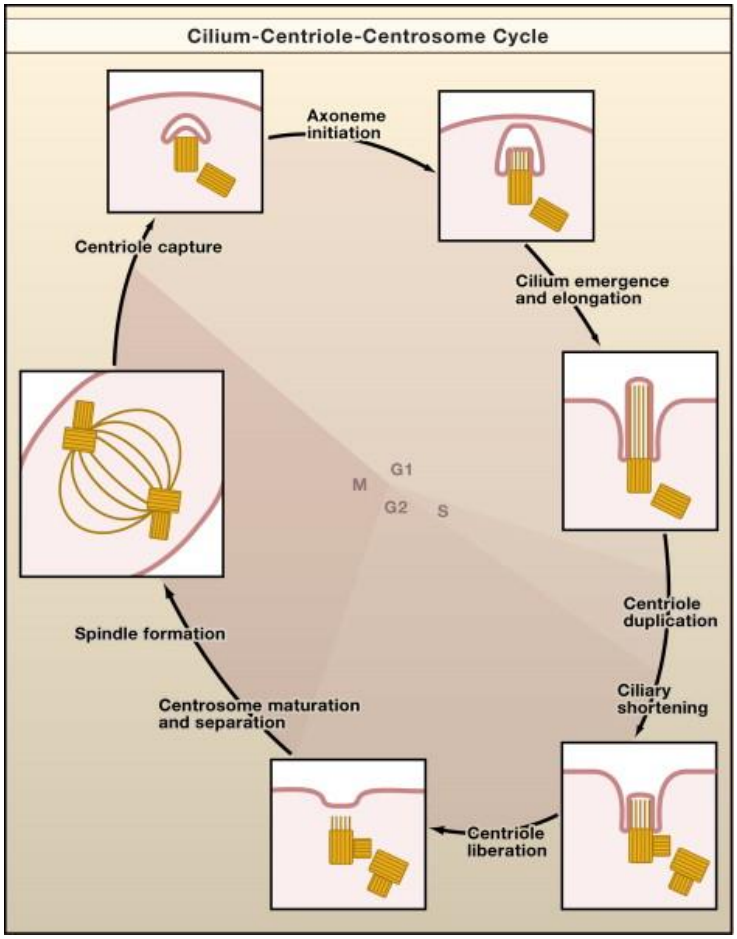

Figure 3. Cilia-centrosome cycle. The primary cilia begins to form upon G0 initiation and resorbs once the cell is signaled to divide again.

CILIARY SIGNALING

The primary cilium functions as a sensor for the cell; it can function as a chemosensor, mechanosensor and osmosensor [5, 13]. The primary cilium houses many signaling receptors, such as patched and smoothened, involved in the hedgehog signaling pathway, and the Wnt ligand lipoprotein related protein (LRP) [17, 18]. The receptors at the ciliary membrane receive chemical signals from the extracellular environment and transmit them intracellularly through a bidirectional process termed intraflagellar transport (IFT), importing and exporting ciliary cargo due to the absence of protein synthesis in the axoneme [13].

The kinesin-2 heterotrimeric complex, consisting of KAP3, KIF3A and KIF3B, contributes to anterograde transport by chaperoning cargo from the base of the ciliary axoneme to the tip (plus end) [19, 20]. Once the anterograde transport proteins reach the distal tips, dynein proteins are activated and chaperone other various proteins and cargo down, towards the base (minus end) of the axoneme during retrograde transport [21, 22]. Primary cilia maintenance is highly dependent on the kinesin-2 complex, however, it is not the only governing component. Many of the IFT proteins and their roles have been investigated, some playing major roles in ciliary formation, maintenance, and resorption [23-25].

Primary cilia have roles in multiple signal transduction pathways, including platelet derived growth factor receptor (PDGFR), hedgehog (Hh), planar cell polarity (PCP) and Wnt signaling. Both the hedgehog transmembrane protein smoothened and

the downstream Wnt protein β-catenin have been localized to the primary cilium [17, 26]. However, the role of the primary cilium in Wnt signaling is largely unknown, except that the state of the cilium affects Wnt-ligand binding and downstream protein activity. Wnt signaling has two major pathways, the canonical and non-canonical pathway. The canonical pathway is initiated when various Wnt ligands, such as Wnt3a, bind to the membrane bound frizzled (Fz) and LRP5/6 receptors [27, 28]. LRP then sequesters disheveled (dsh) and axin to the plasma membrane, subsequently breaking apart the destruction complex (made up of axin, adenomatous polyposis coli (APC), and glycogen synthase kinase 3β (GSK3β)) that degrades β-catenin [29-31]. β-catenin then accumulates and is able to bind to primary cilia and/or translocate into the nucleus where it then binds to T-cell factor (TCF)/ lymphoid enhancer factor (LEF) and activates downstream targets, such as cyclin D1 and c-myc [26, 32]. When the canonical Wnt pathway is not active, non-canonical Wnt signaling takes place, modulating planar cell polarity (PCP) and calcium signaling [33]. The Wnt5A ligand binds to receptor tyrosine kinase-like orphan receptor 2 (ROR2) and Fz, recruiting (dsh), which activates ras homolog A (RhoA) and ras-related C3 botulinum toxin substrate1 (RAC1) [34-36]. RAC1 continues the signaling cascade controlling cell polarity [34, 36]. Additionally, when Wnt binds to ROR2, calcium is released, allowing for nuclear factor of activated T-cells (NFAT) controlled calcium-mediated transcriptional regulation and increased levels of nemo-like kinase (NLK) which inhibits TCF/LEF transcriptional activation [33].

Proteins such as polycystin-1 (PC1) also localize to the primary cilium, sensing fluid flow, touch, pressure and vibration, contributing to the primary cilium's mechanical role [37-39]. Mutations arising on the polycystic kidney disease-1 (*PKD1*) gene (encoding PC1), lead to autosomal dominant polycystic kidney disease (ADPKD), a multisystemic disorder resulting in renal, liver and pancreatic cysts. Mutations in the *PKD2* gene, encoding PC2 can also lead to ADPDK. Additionally, polycystin-2 (PC2, TRPP2) localizes to the cilium and complexes with transient receptor potential cation channel subfamily V member 4 (TRPV4) to heterodimerize, forming an ion channel complex which senses and reacts to changes in osmolarity and can modulate calcium influx [37, 38, 40]. It has been hypothesized that the extracellular domains of PC1 that sense fluid flow in the kidney, also activate PC2 [37]. Once the polycystins heterodimerize, a calcium-permeable cation channel is generated and opens, allowing for calcium influx, increasing intracellular calcium concentrations [41]. Nauli et al. 2008 determined that the extracellular movement of calcium is the primary trigger to the mechanical stimulation response [41]. Calcium then functions to increase cyclic adenosine monophosphate (cAMP) levels, regulating phosphodiesterase 1 (PDE1) protein inhibition (known to be high in individuals with PKD) [42, 43]. In PDK individuals, calcium influx is dysregulated, allowing for increases in PDE1, which subsequently activates MAPK signaling, resulting in increased proliferation and cyst progression [43].

CILIOPATHIES

There are over 800 proteins that function in the formation and stability of the primary cilium. When major proteins and genes are dysregulated, they can lead to the dysfunction of ciliary processes that can cause a variety of diseases, also known as ciliopathies. For example, alteration and dysfunction of the *BBS1*, *BBS4*, *BBS8* genes contribute to Bardet-Biedl syndrome, dysfunction of ARL13b promotes Joubert Syndrome and kinesin proteins such as KIF3a, involved in anterograde IFT, contributes to PKD [24, 44-46]. Dysfunction of other genes, such as *APC* can lead to Gardner's syndrome, a subtype of familial polyposis coli (FAP), resulting in extracolonic manifestations such as congenital hypertrophy of the retinal pigmented epithelium (CHRPE), osteomas and cysts, deeming it a cilia-related disorder [47, 48]. However, the majority of other dysregulated genes affecting the primary cilium show phenotypic effects of the kidney, including the von-Hippel Lindau (*VHL*) gene, whose dysregulation leads to renal cysts and often tumorigenesis [49-51]. The protein of *VHL* (pVHL) is an E3 ubiquitin ligase, sequestering substrates and tagging them for degradation [52]. pVHL is known to interact with many proteins found to localize at the primary cilia, including HIF-1α, AURKA and Jade-1, all playing important roles in various ciliary processes, making *VHL* a crucial tumor suppressor gene [51, 53, 54].

CHAPTER II

LINKING β-CATENIN TO PRIMARY CILIA VIA AURKA TRANSCRIPTIONAL ACTIVATION IN RENAL CELL CARCINOMA*

INTRODUCTION

Mutations in the *von Hippel-Lindau* (*VHL*) gene are associated with the most aggressive histopathologic subtype of renal cell carcinoma (RCC): clear cell renal cell carcinoma (ccRCC) [49]. Individuals with germline defects are susceptible to second-hit mutations resulting in inactivation of both alleles of this critical tumor suppressor [55]. pVHL has numerous cellular functions, with its role as the recognition component of a multiprotein ubiquitin degradation complex being most well characterized [52]. Hypoxia-inducible factor-α (HIF-α) is perhaps the most well studied target of VHL's E3 ligase activity, linking loss of pVHL with cellular proliferation and angiogenesis [56, 57]. In a non-proteasomal role, pVHL has been shown to stabilize microtubules and regulate cell cycle progression [13, 58, 59,60]. More recently, loss of VHL has been linked to loss of primary cilia which is thought to be the driver for both cyst and tumor formation in the setting of VHL deficiency [12, 61, 62, 63, 64]. Primary cilia are microtubule-based organelles on the apical surface of renal epithelial cells that are involved in sensing environmental cues and regulating several cell signaling pathways [65-68].

---

*Reprinted with permission from "β-catenin Links von Hipple-Lindau to Aurora A and Loss of Primary Cilia in Renal Cell Carcinoma" by Dere R, Perkins AL, Bawa-Khalfe T, Jonasch D, Walker CL, 2015. *JASN*, **26** (3) 553-564

The appreciation for the central role of the primary cilium in cellular homeostasis has given rise to the identification of a new class of disorders, referred to as ciliopathies [69]. In several ciliopathies, loss of tumor suppressors, such as *VHL*, results in loss of primary cilia and initiation of disease [60]. The mitotic kinase Aurora kinase A (AURKA) was recently reported to have a novel nonmitotic activity. AURKA was shown to interact with enhancer of filamentation 1 (HEF1/NEDD9), to phosphorylate and activate histone deacetylase 6 (HDAC6). Activation of HDAC6, a tubulin deacetylase, causes disassembly of the microtubule axoneme of the primary cilia [14]. In the context of RCC, AURKA levels are elevated in ccRCC and in high-grade renal tumors [50, 51, 70]. In another report, AURKA was suggested to be a specific target of HIF-1α in the setting of VHL deficiency, although the exact mechanism linking HIF-1α and AURKA activation was not explored. VHL has other targets in addition to HIF [71]. For example, VHL interacts with and stabilizes Jade-1 which also functions as an E3 ligase that regulates β-catenin levels [72-74]. In the case of VHL deficiency, Jade-1 levels are significantly reduced leading to increased levels of β-catenin [53]. This led us to hypothesize that AURKA may be upregulated because of transcriptional activation by β-catenin in the setting of VHL deficiency. Our studies show that AURKA signaling to HDAC6 is modulated by β-catenin–driven transcription, and rather than increasing AURKA transcription, HIF-1α inhibits AURKA expression via repression of β-catenin itself. Increased AURKA expression after loss of VHL leads to a decrease in the number and length of primary cilia. Inhibition of AURKA expression using a β-catenin inhibitor, iCRT14, was able to rescue ciliary defects associated with VHL deficiency, suggesting

that interventions targeting β-catenin could have efficacy for reversing the effects of VHL loss.

RESULTS

AURKA Is Elevated in VHL-Deficient Cell Lines

We examined AURKA expression in a panel of VHL-proficient (Caki-1) and VHL-deficient (786-O, 769-P, and A-498) quiescent RCC cell lines. As shown in Figure 4A, AURKA mRNA levels were significantly higher in VHL-deficient cells compared with VHL positive cells. Commensurate with elevated mRNA, we also observed higher AURKA protein levels in the VHL-null RCC cell lines (Figure 4B). Because AURKA interacts with HEF1/NEDD9 to activate HDAC6, we also examined levels of HEF1 and HDAC6 in these cells [14]. Both HEF1 (3- to 40-fold) and HDAC6 (3- to 5-fold) were increased in cells lacking VHL (Figure 4B). Xu et al. previously reported that AURKA and HEF1 are elevated in VHL-deficient, RCC10, and RCC4 cells, and suggested that this increase was due to stabilization of HIF-1α [71]. However, in contrast with the RCC cell lines in that report, HIF-1α levels were previously characterized to be virtually nonexistent in the 786-O, 769-P, and A-498 cells [75]. This would suggest that an alternate mechanism exists in VHL-deficient cells to increase AURKA and HEF1 expression and cause cilia disassembly. To evaluate whether HEF1 could directly modulate AURKA expression, we knocked down HEF1 in VHL-null 786-O cells and found that AURKA levels remained unchanged after loss of HEF1 (Figure 4C). These data indicate that modulating HEF1 alone in these cells was unable to regulate AURKA expression. Using quiescent normal human retinal pigmented epithelial (hTERT RPE-1) cells, a well characterized

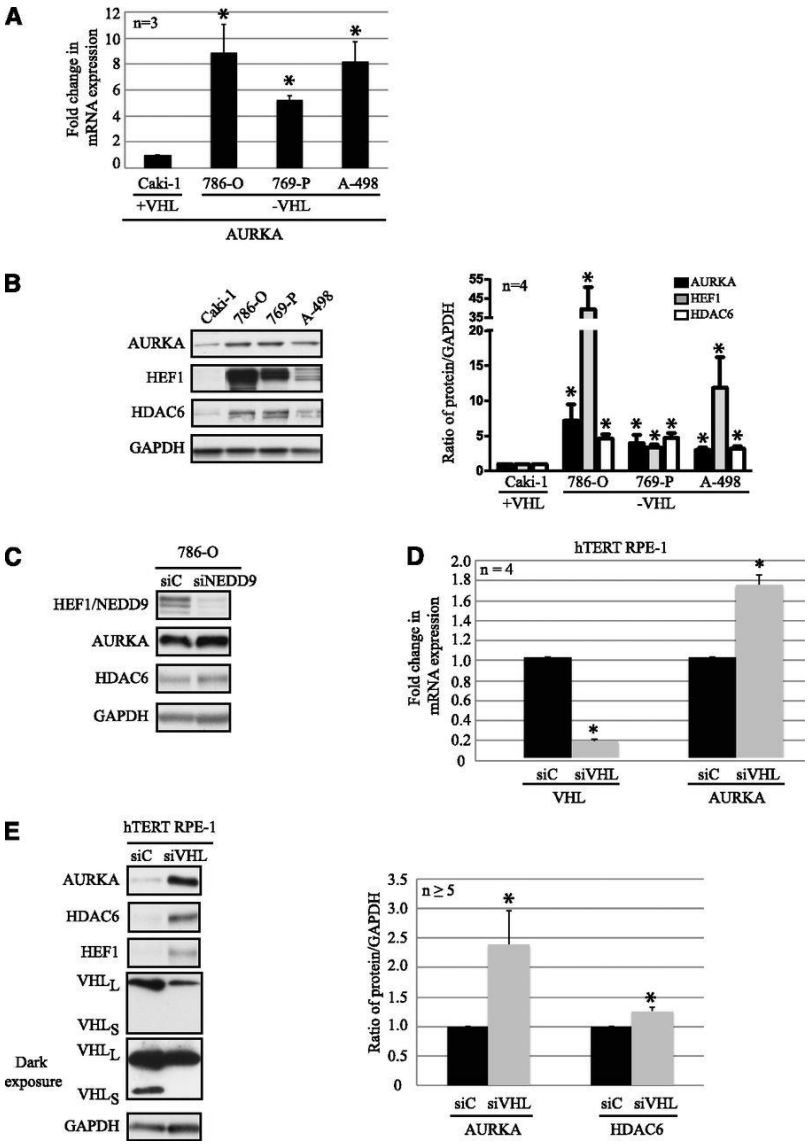

Figure 4. AURKA expression and signaling to HDAC6 is elevated in RCC. (A) RT-PCR analyses of AURKA mRNA expression in VHL-proficient (Caki-1) or VHL-deficient (786-O, 769-P, and A-498) RCC cells, normalized to Caki-1 (P<0.01). (B) Lysates from VHL-proficient (Caki-1) or VHL-deficient (786-O, 769-P, and A-498) RCC cells are probed with the indicated antibodies (left). Densitometric analyses of protein expression normalized to GAPDH expression from four independent experiments, plotted as graphs showing AURKA (black bars), HEF1 (grey bars), and HDAC6 (white bars) expression compared with expression in the Caki-1 cells (P<0.05). (C) Lysates from 786-O cells expressing the siC nontargeting scrambled control or siNEDD9 are probed with NEDD9, AURKA, HDAC6, and GAPDH antibodies. (D) RT-PCR analyses of hTERT RPE-1 cells transfected with a nontargeting control siC (black bars) or siVHL (grey bars) showing fold-changes in VHL and AURKA transcript levels as indicated (P<0.01). (E) Lysates from normal hTERT RPE-1 cells expressing siC or siVHL are immunoblotted for the indicated antibodies. Densitometric analyses from at least five independent experiments are shown as graphs indicating levels of AURKA and HDAC6 in cells expressing siC (black bars) or siVHL (grey bars) (P<0.01). *Statistically significant differences.

ciliogenesis model, we confirmed that knocking down VHL using small interfering RNA (siRNA) resulted in increased AURKA and HEF1 expression, mimicking our observations in VHL-null RCC cell lines. RT-PCR showed an 80% efficiency of knockdown in cells expressing VHL-specific siRNA compared with scrambled control (Figure 3D).With VHL knockdown, we observed a corresponding increase (80%) in AURKA mRNA (Figure 3D) and protein levels (Figure 3E). Quantitation revealed a significant (.2-fold) increase in AURKA, and a smaller but statistically significant increase in HDAC6 (Figure 3E, graph). Importantly, HDAC6 expression levels are used as an indirect measure of its activity; thus, the modest increase in HDAC6 expression (25%) could potentially result in much higher HDAC6 activity [14].

HIF-1α Inhibits AURKA Expression in Normal Epithelial Cells

To further explore whether HIF-1α was involved in upregulating AURKA expression, we knocked down HIF-1α (siHIF1α) in hTERT RPE-1 cells. RT-PCR confirmed a 90% decrease in HIF-1α mRNA (Figure 5A), and protein levels (Figure 5B). We found that AURKA mRNA was significantly higher with HIF-1α knockdown compared with the non-targeting control (Figure 4A), accompanied by a 5-fold increase in AURKA protein levels (Figure 5B). These data led us to hypothesize that rather than increasing AURKA expression, HIF-1α decreased expression of this kinase. We used two pharmacologic hypoxia mimetics, dimethyloxalylglycine and defroxamine, to promote accumulation of HIF-1α. Initially, dose-response experiments were conducted to optimize the concentration of the hypoxia mimetics to stabilize HIF-1α with minimal

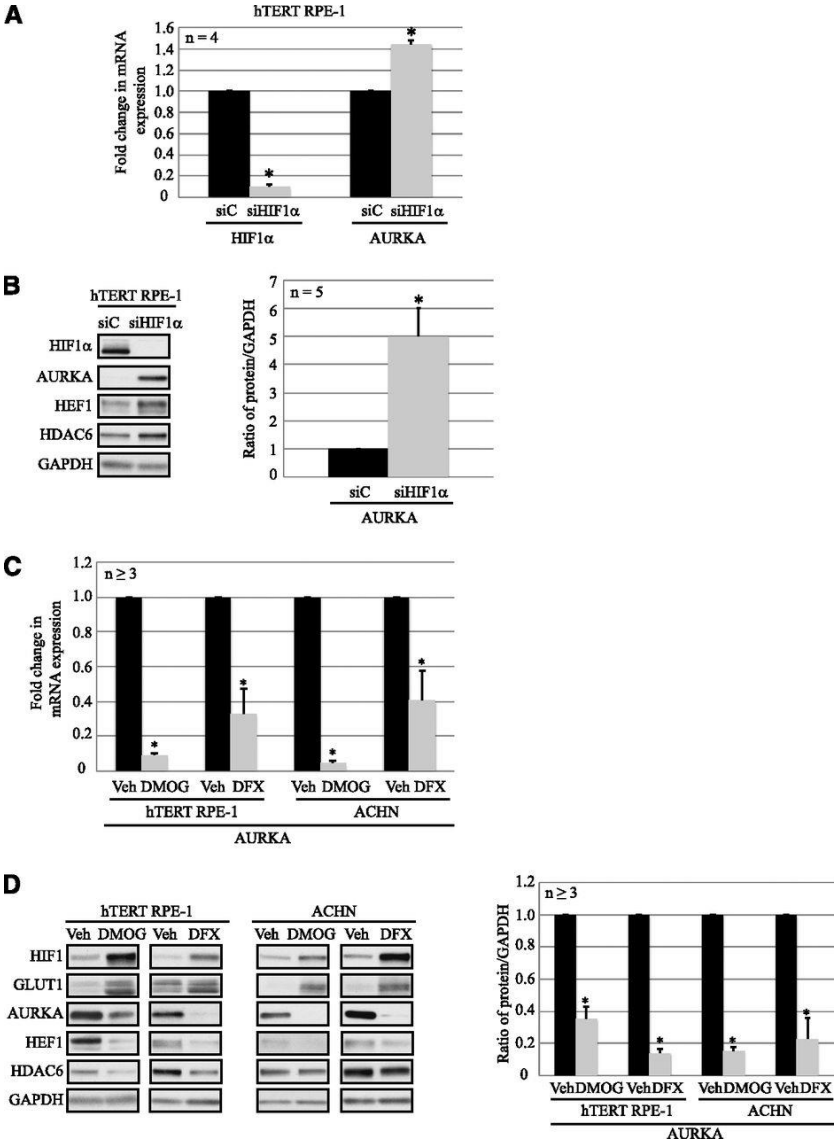

Figure 5. HIF-1α inhibits AURKA expression in epithelial cells. (A) mRNA expression of HIF-1α and AURKA from hTERT RPE-1 cells transfected with the siC nontargeting (scrambled) control (black bars) or siHIF-1α (grey bars) (P<0.01). (B) Lysates prepared from hTERT RPE-1 cells transfected with siC (black bars) or siHIF-1α (grey bars) are analyzed by immunoblotting with the indicated antibodies. Densitometric analyses from five independent experiments showing AURKA protein expression normalized to GAPDH are denoted in the graph (P<0.01). (C) RT-PCR analyses of AURKA mRNA from hTERT RPE-1 and ACHN cells treated with water (vehicle; black bars), DMOG (1 mM; grey bars), or defroxamine (250 μM; grey bars) as indicated (P<0.01). (D) Cell lysates from hTERT RPE-1 and ACHN cells treated with vehicle (black bars), DMOG (1 mM; grey bars), or DFX (250 μM; grey bars) are immunoblotted with the indicated antibodies. Densitometric analyses showing protein expression normalized to GAPDH from at least three independent replicates are shown in the graph (right) (P<0.01). *Statistically significant differences.

toxicity to the cells. In hTERT RPE-1 and VHL-proficient ACHN RCC cells treated with dimethyloxalylglycine (1 mM) or defroxamine (250 μM), stabilization of HIF-1α was confirmed by increased HIF-1α and Glut1 (a downstream target of HIF-1α) protein levels (Figure 5D). AURKA expression decreased at the mRNA (Figure 5C) and protein levels (Figure 5D) with both inhibitors. We also observed a significant decrease in HDAC6 and HEF1 protein expression (Figure 5D) in response to stabilized HIF-1α. These data support the hypothesis that HIF-1α inhibits both AURKA and HEF1 expression.

Loss of HIF-1α and VHL Activates β-catenin

Kaidi et al. 2007 found that in colorectal carcinoma cells HIF-1α inhibited β-catenin–driven transcription, and another study reported Jade-1, a protein stabilized by VHL, targeted β-catenin for proteasome-mediated degradation [72, 76]. These reports lead us to hypothesize that HIF-1α inhibited AURKA expression via modulation of β-catenin in VHL-deficient cells. First, to determine whether HIF-1α inhibited β-catenin activity, we examined RNA levels of two well established β-catenin targets (cyclin D1 and c-myc) after HIF-1α knockdown, and we observed increased expression of both the mRNA (Figure 6A). Conversely, use of hypoxia mimetics to stabilize HIF resulted in a significant decrease in cyclin D1 and c-myc mRNA (Figure 6B) in both hTERT RPE-1 and. ACHN cells.

Next, subcellular fractionation of VHL proficient and VHL-deficient RCC cells revealed accumulation of nuclear β-catenin in VHL-null RCC cells compared with VHL

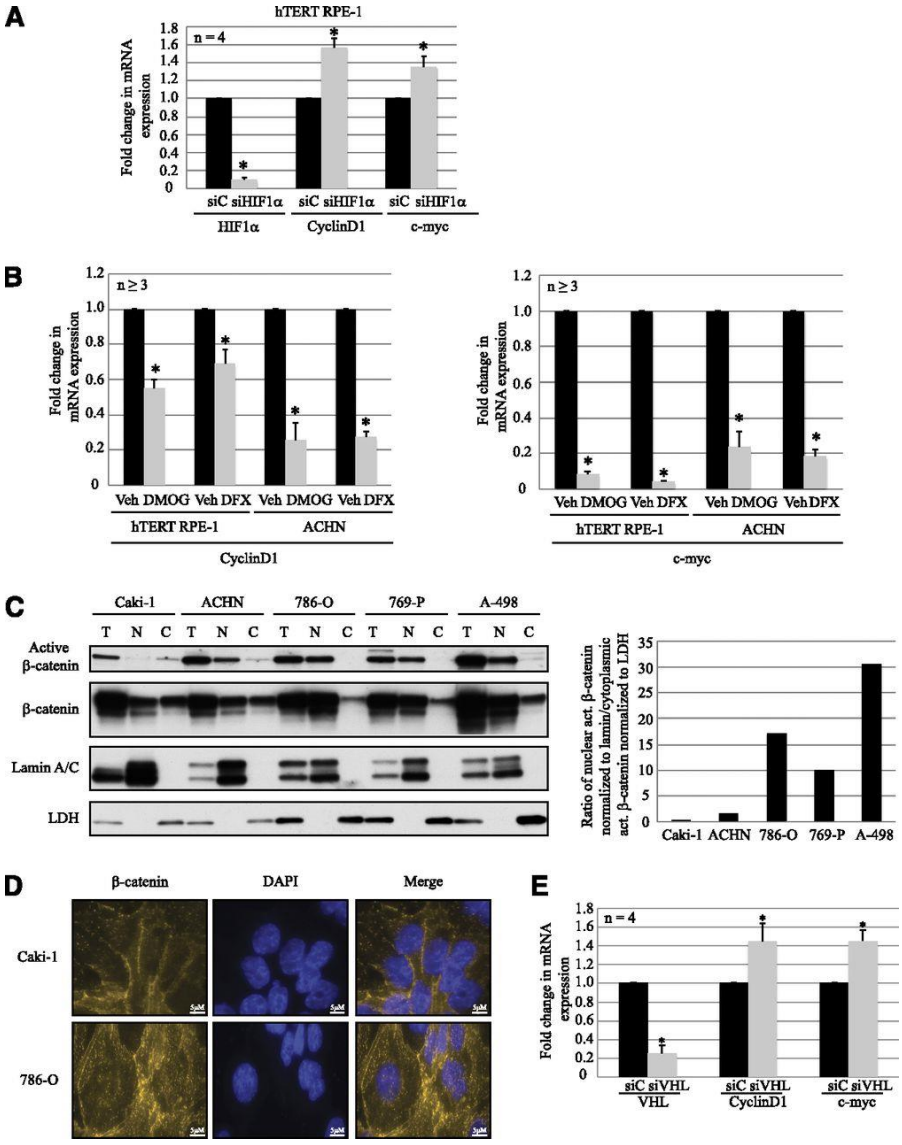

Figure 6. Loss of HIF-1α and VHL promotes activation of β-catenin. (A) RT-PCR analyses of hTERT RPE-1 cells expressing nontargeting control siC (black bars) or siHIF-1α (grey bars), showing mRNA levels of HIF-1α, CyclinD1, and c-myc (P<0.01). (B) RT-PCR analyses showing CyclinD1 (left) and c-myc (right) transcript levels in hTERT RPE-1 and ACHN cells treated with vehicle (black bars) or hypoxia mimetics DMOG (1 mM; grey bars) or DFX (250 μM; grey bars) as indicated (P<0.01). (C) Subcellular fractionation of VHL-proficient (Caki-1 and ACHN) and VHL-null (786-O, 769-P, and A-498) RCC cells, immunoblotted with the indicated antibodies (Lamin A/C, nuclear marker; LDH, cytoplasmic marker; T, whole cell extract; N, nuclear; C, cytoplasmic). Densitometric analyses (right) of the blots (left) indicating a ratio of activated β-catenin in the nuclear fraction (normalized to nuclear marker Lamin A/C) to the levels in the cytoplasmic fraction (normalized to cytoplasmic marker LDH). (D) Immunofluorescence staining of Caki-1 and 786-O cells using β-catenin (yellow) antibody. The nuclei are counterstained with DAPI (blue). (E) RT-PCR analyses of hTERT RPE-1 cells expressing nontargeting control siC (black bars) or siVHL (grey bars), showing mRNA expression levels of VHL, CyclinD1, and c-myc (P<0.01). *Statistically significant differences.

-positive RCC cells (Figure 6C). Nuclear active β-catenin is dephosphorylated and drives transcription of its downstream targets [76]. In VHL-deficient RCC cells, we found that the ratio of activated β-catenin in the nucleus (when normalized to nuclear marker expression) to that in the cytoplasm (normalized to cytoplasmic marker expression) is higher than the same ratio in VHL-proficient cells (Figure 6C, graph). Similarly, immunofluorescence showed enhanced nuclear localization of β-catenin in VHL-deficient (786-O) cells compared with the VHL-positive (Caki-1) cells (Figure 6D).We further confirmed activation of β-catenin after loss of VHL in the hTERT RPE-1 cells by measuring cyclin D1 and c-myc transcript levels, which were elevated in VHL-deficient cells (Figure 6E).

AURKA Expression Is Regulated by β-catenin–Driven Transcription

Because we observed that β-catenin-driven transcription was repressed when HIF-1α was stabilized, as was AURKA expression, we hypothesized that AURKA transcription was regulated by β-catenin. To investigate the role of β-catenin in modulating AURKA, we overexpressed β-catenin in hTERT RPE-1 cells, and consequentially observed increased AURKA mRNA (Figure 7A), and protein levels (Figure 7B). By contrast, knocking down β-catenin or T-cell factor 1 (TCF-1) showed decreased AURKA mRNA (Figure 7, C and E) and protein (Figure 7, D and F) levels. To determine whether β-catenin was directly modulating AURKA transcription, we

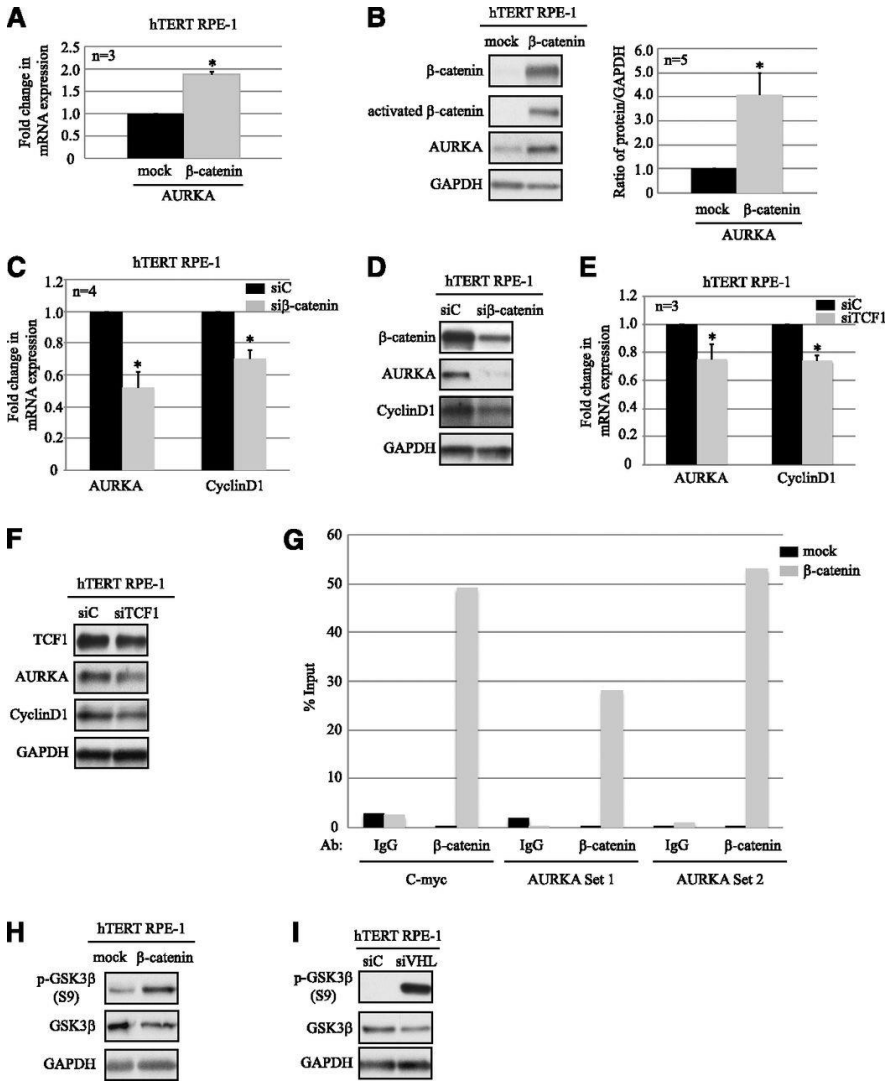

Figure 7. *β*-catenin drives AURKA expression. (A) RT-PCR analyses showing AURKA mRNA levels in hTERT RPE-1 cells overexpressing *β*-catenin construct (grey bar) or a mock transfection control (black bar) ($P<0.01$). (B) Lysates from hTERT RPE-1 cells overexpressing *β*-catenin immunoblotted for the indicated antibodies (left), and densitometric analyses (right) ($P<0.01$). Black bars (mock) and grey bars (*β*-catenin overexpression). (C) mRNA expression of AURKA and CyclinD1 from hTERT RPE-1 cells transfected with a siC (black bars) or si*β*-catenin (grey bars) ($P<0.01$). (D) Representative blots of lysates prepared from hTERT RPE-1 cells transfected with siC or si*β*-catenin are analyzed by immunoblotting with the indicated antibodies ($n=4$). (E) mRNA expression of AURKA and CyclinD1 from hTERT RPE-1 cells transfected with a siC (black bars) or siTCF-1 (grey bars) ($P<0.05$). (F) Representative blots of lysates prepared from hTERT RPE-1 cells transfected with siC or siTCF-1 are analyzed by immunoblotting with the indicated antibodies ($n=3$). (G) ChIP assay in hTERT RPE-1 cells transfected with a *β*-catenin construct or a mock transfection control demonstrating direct binding of *β*-catenin to the AURKA gene promoter. ChIP is performed with either IgG or *β*-catenin antibodies followed by RT-PCR for using primers for the regions as indicated. (H) Representative immunoblots from lysates generated by overexpressing *β*-catenin in hTERT RPE-1 cells probed with phospho-GSK3*β* (S9), GSK3*β*, and GAPDH antibodies. (I) Immunoblot analyses of hTERT RPE-1 cells with VHL knockdown (siVHL) probed with the indicated antibodies. GAPDH serves as the loading control. *Statistically significant differences.

performed chromatin immunoprecipitation (ChIP) analyses in hTERT RPE-1 cells overexpressing β-catenin. ChIP analyses revealed that β-catenin directly recognized and immunoprecipitated regions of the AURKA promoter, similar to reports in multiple myeloma (Figure 7G), demonstrating that AURKA is a direct target of β-catenin. The cellular activity of β-catenin is regulated by glycogen synthase kinase-3β (GSK3β), which is part of the β-catenin destruction complex [77, 78]. In addition, AURKA was reported to phosphorylate GSK3β at S9 in gastric cancer, resulting in the inactivation of this kinase, thereby increasing levels of activated β-catenin [79]. Hence, we examined phosphorylation of GSK3β (S9) in hTERT RPE-1 cells overexpressing β-catenin and elevated AURKA, and observed increased phosphorylation of GSK3β at S9 (Figure 7H). Similarly, GSK3β phosphorylation increased in cells after VHL knockdown (Figure 7I). These data directly link elevated AURKA to β-catenin–driven transcription.

Elevated AURKA Expression Leads to Abnormal Primary Cilia in VHL-Deficient Cells

AURKA causes disassembly of the primary cilium via activation of HDAC6 [14]. Enhanced AURKA expression after loss of VHL lead us to examine primary cilia in hTERT RPE-1 cells with VHL knockdown. In contrast with a previous report by Thoma et al. in which loss of VHL in primary human cells failed to elicit a ciliary defect, we found that knocking down VHL in the hTERT RPE-1 cells showed a significant shortening of cilia length compared with control cells (Figure 8A) [12]. Three independent replicates revealed that in cells deficient for VHL, there was a significant nearly 2-fold increase in cells that failed to make primary cilia (Figure 8B). In cells that

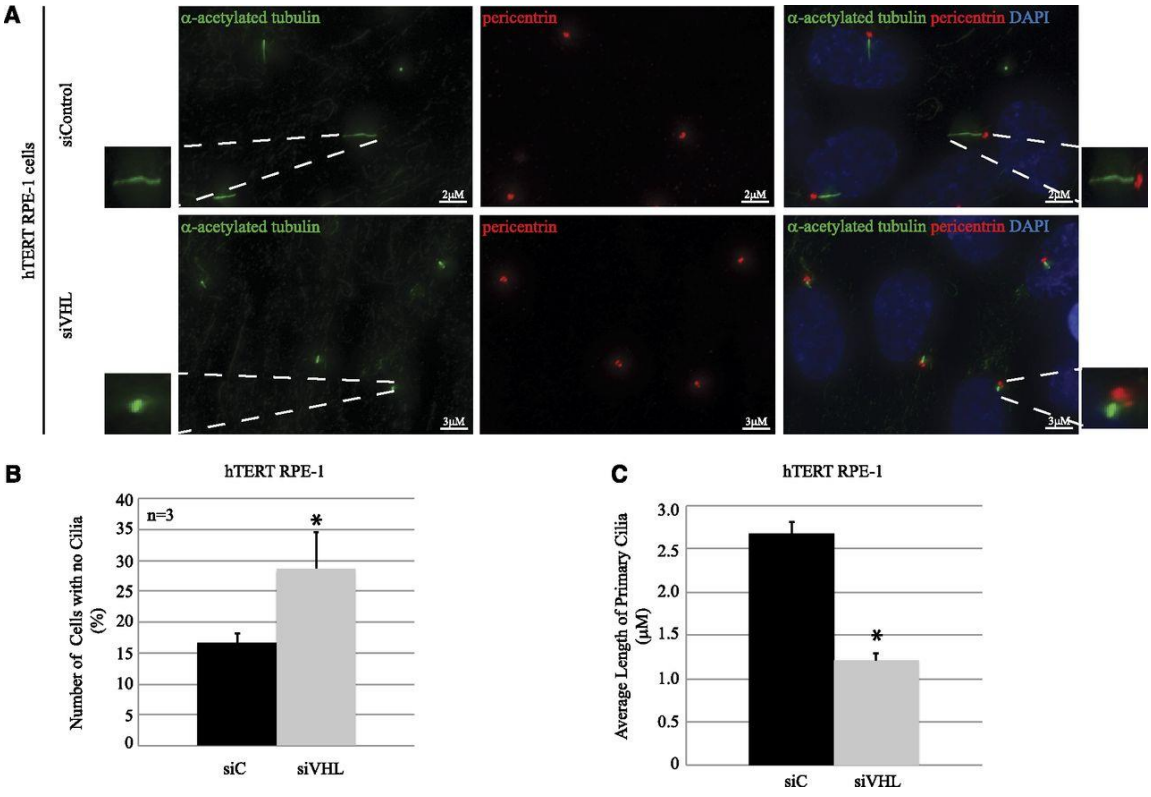

Figure 8. Loss of VHL results in shortening of primary cilia. (A) Immunofluorescence staining of hTERT RPE-1 cells expressing siC or siVHL using acetylated α-tubulin (cilia marker, green) and pericentrin (basal body marker, red). The nuclei are counterstained with DAPI (blue). Enlarged panels show higher magnification of primary cilia. (B) Immunofluorescence images are analyzed using Imaris software to quantitate the number of cells that failed to form primary cilia from >100 individual hTERT RPE-1 cells transfected with siC (black bars) or siVHL (grey bars). Data from three independent replicates (each >100 cells) are denoted as a percentage of cells without cilia (P<0.01). (C) Immunofluorescence images are analyzed using Imaris software to measure the length of the primary cilia from >150 individual hTERT RPE-1 cells transfected with siC (black bars) or siVHL (grey bars). A representative experiment is shown (P=3.4×10^{-22}). *Statistically significant differences.

retained cilia after VHL knockdown, we observed a 50%–60% shortening of cilia length (representative experiment shown in Figure 8C). Importantly, these estimates are likely modest because cilia measurements were performed on a population basis, which would include both transfected and non-transfected cells.

Inhibition of β-catenin Regulated AURKA Transcription Rescues Aberrant Ciliogenesis in VHL Deficient Cells

Because our data link β-catenin to high AURKA in VHL deficient cells, and the resultant loss of primary cilia, we assessed the efficacy of a β-catenin inhibitor iCRT14 to rescue both elevated AURKA and cilia defects in the setting of VHL deficiency. iCRT14 is a potent and selective inhibitor of β-catenin responsive transcription with no direct effect on β-catenin or its cytoplasmic interactions with junction proteins [80, 81]. Initial dose-response experiments showed maximal β-catenin inhibition with minimal toxicity at a dose of 15 μM. hTERT RPE-1 cells with VHL knockdown showed higher AURKA mRNA (Figure 9A) compared with cells with scrambled control when treated with vehicle (EtOH). Treatment with iCRT14 decreased AURKA expression showing an 80% decrease in AURKA mRNA (Figure 9A). Levels of the β-catenin targets cyclin D1 and c-myc mRNA were assessed as positive controls for iCRT14 inhibition of β-catenin transcription (Figure 9A). The 3-fold decrease in AURKA expression was accompanied by a 2-fold decrease in HDAC6 protein in VHL-deficient cells treated with iCRT14 (Figure 9B).

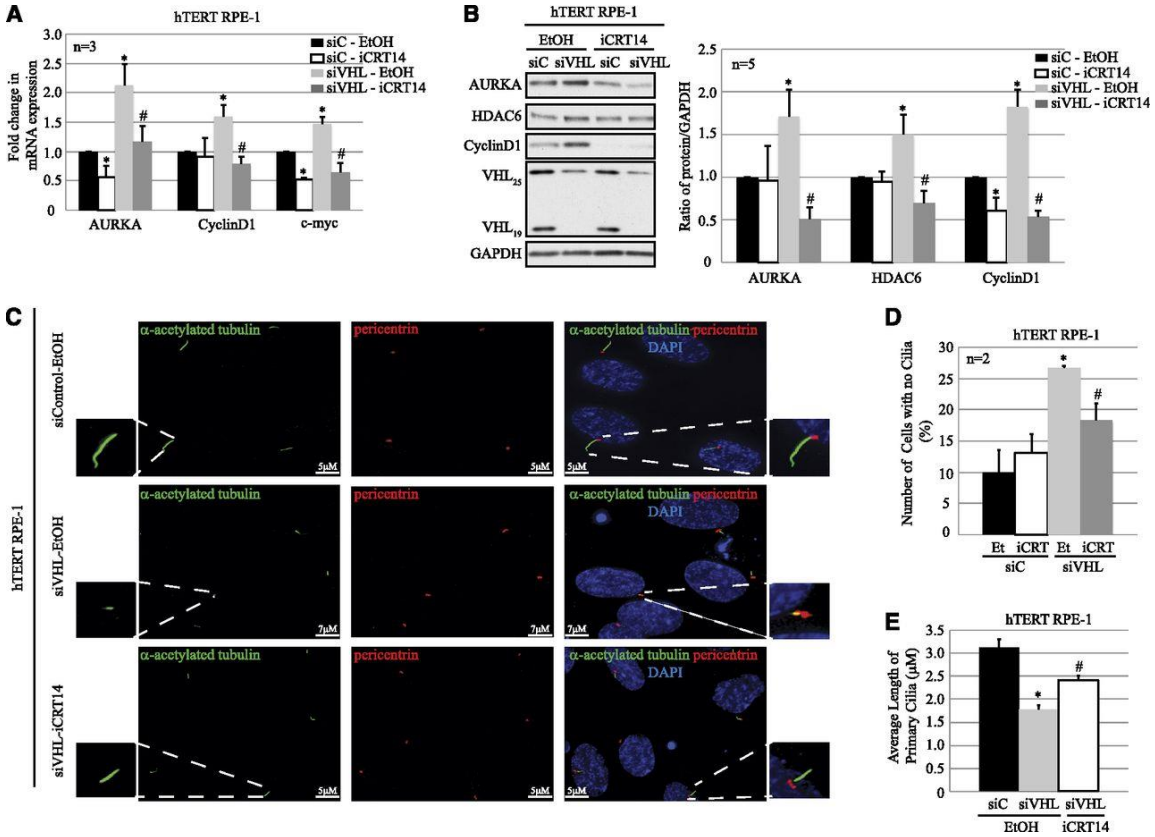

Figure 9. Inhibition of β-catenin responsive transcription rescues the ciliary defect in epithelial cells after acute loss of VHL. (A) RT-PCR analyses of hTERT RPE-1 cells expressing siC treated with vehicle (EtOH; black bars) or iCRT14 (15 μM; white bars), or siVHL treated with either vehicle (EtOH; light grey bars) or iCRT14 (15 μM, dark grey bars) showing AURKA, CyclinD1, and c-myc mRNA transcript levels as indicated (P<0.05). (B) Immunoblot analyses from hTERT RPE-1 cells transfected with either siC treated with EtOH (black bars) or iCRT14 (15 μM; white bars) or siVHL treated with EtOH (vehicle; light grey bars) or iCRT14 (15 μM; dark grey bars) probed with the indicated antibodies (left). Densitometric analyses showing protein expression normalized to GAPDH (loading control; right) (P<0.05). (C) Immunofluorescence staining of hTERT RPE-1 cells expressing siC or siVHL, treated with EtOH (vehicle) or iCRT14 (15 μM), using acetylated α-tubulin (cilia marker, green) and pericentrin (basal body marker, red). The nuclei are counterstained with DAPI (blue). A single primary cilium is shown in the enlarged panels. (D) Immunofluorescence images are analyzed using Imaris software to quantitate the number of cells that failed to make primary cilia from >100 individual hTERT RPE-1 cells transfected with siC treated with EtOH (black bars) or iCRT14 (white bars) or siVHL treated with EtOH (light grey bars) or iCRT14 (dark grey bars). Data from three independent replicates (each >100 cells) are denoted as a percentage of cells without cilia (P<0.01). (E) Immunofluorescence images are analyzed using Imaris software to measure the length of the primary cilia from >150 individual hTERT RPE-1 cells transfected with siC treated with EtOH (black bars) or siVHL treated with EtOH (grey bars) or iCRT14 (white bars). A representative experiment is shown (P<0.01). *Statistically significant differences compared with siC-EtOH; #Statistically significant differences between siVHL-EtOH and siVHL-iCRT14 treatment groups.

Importantly, we wanted to evaluate the ability of iCRT14 to rescue the ciliary defect associated with VHL deficiency. In cells with VHL knockdown, treatment with iCRT14 rescued the ciliary defect associated with VHL loss (Figure 9C). We found that fewer cells lacked primary cilia (Figure 9D), and those with cilia had longer primary cilia (Figure 9E) after iCRT14 treatment compared with the vehicle-treated controls. These data show that decreasing β-catenin–driven transcription of AURKA is sufficient to promote ciliogenesis in the setting of VHL deficiency. Because iCRT14 successfully reduced AURKA after acute loss of VHL, we asked whether inhibition of catenin responsive transcription would also rescue AURKA signaling in the setting of RCC. We treated VHL-null 786-O and 769-P RCC cell lines (with high AURKA) with iCRT14 (15 μM), and observed a significant reduction in AURKA expression (Figure 10A) in these cells. Concomitant decrease in cyclin D1 and c-myc transcript levels served as a positive control for inhibitor treatment with HDAC6 serving as a negative control. A corresponding reduction in AURKA and HDAC6 protein levels was observed in response to iCRT14 treatment, indicating successful rescue of AURKA activation of HDAC6 (Figure 10B). As shown in Figure 10C, these data suggest a model in which inhibiting β-catenin could serve as a promising new avenue to reverse elevated AURKA and prevent loss of primary cilia in the setting of VHL-deficient ccRCC.

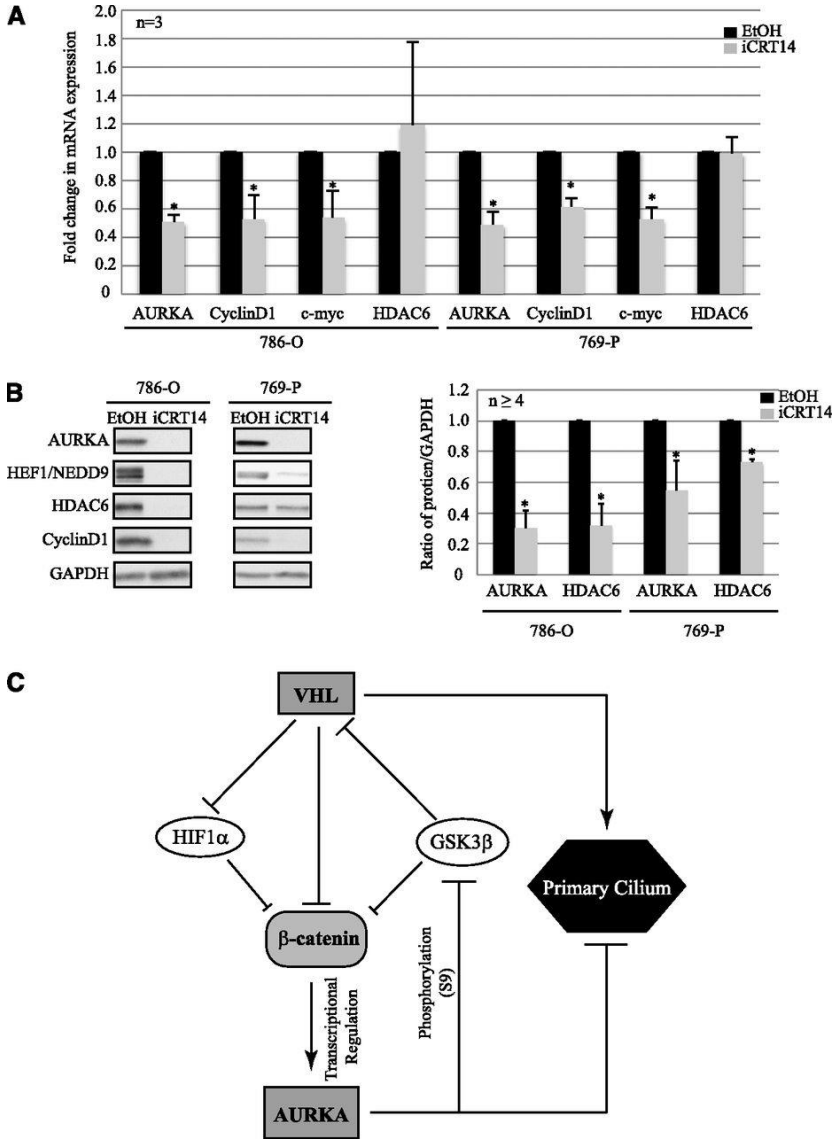

Figure 10. iCRT14 rescues aberrant AURKA signaling in RCC cell lines. (A) RT-PCR analyses showing AURKA, CyclinD1, c-myc, and HDAC6 mRNA expression in VHL-null, 786-O, and 769-P RCC cell lines treated with vehicle (EtOH; black bars) or iCRT14 (15 μM; grey bars) (P<0.05). (B) Immunoblot analyses from 786-O and 769-P RCC cells treated with EtOH (black bars) or iCRT14 (grey bars), probed with the indicated antibodies (left). The graph (right) represents densitometric analyses from at least four independent replicates showing levels of protein expression normalized to GAPDH expression (loading control) (P<0.05). (C) Model for β-catenin regulation of AURKA in VHL-deficient cells. *Statistically significant differences.

DISCUSSION

The ccRCC variant arises from loss of VHL, and is associated with loss of primary cilia [49, 60, 61]. Ciliary defects are causally linked to renal cysts and VHL disease progression [60]. Although recent studies demonstrated elevated levels of AURKA in the setting of RCC, the exact mechanism for dysregulated AURKA in this setting is not clearly understood [50, 51, 81, 82]. Our results link β-catenin–driven transcription to regulation of AURKA and loss of primary cilia in VHL-null RCC. Increased AURKA expression in the setting of VHL deficiency decreased cilia formation and inhibition of β-catenin, decreased AURKA expression, and rescued ciliogenesis in the setting of VHL deficiency. HIF-1 was previously shown to bind HIF responsive elements in the promoter of AURKA in liver cells, resulting in its enhanced expression in hepatocellular carcinoma [83, 84]. Although a previous report showed a correlation between HIF-1 and AURKA levels in HIF-1–positive RCC cell lines our data show that AURKA expression is inhibited by HIF-1α in normal and RCC cell lines [71]. This could arise from reduced binding of HIF to the AURKA HIF responsive element as recently observed in breast cancer cell lines [85]. Alternately, it may suggest the existence of an alternate pathway as previously reported for colorectal carcinoma, in which HIF-1α bound to β-catenin precluding its association with T cell factor to prevent activation of its downstream targets [76]. High HIF-1α levels are associated with unfavorable prognosis in most cancers; however, patients with high HIF-1α expression have a better prognosis in ccRCC. Our studies showing inhibition of β-catenin regulated

AURKA by HIF-1α validate the improved survival by upregulated HIF-1α in ccRCC. Recent studies also highlight the critical role of HIF-2α, a renal oncoprotein necessary and sufficient in the pathology of VHL, in activating β-catenin–driven transcription [86-88]. Similar to a previous report that found HIF-1α and HIF-2α as having opposing functions in regulating c-myc signaling, it would be interesting to define the relative contributions of HIF-1α and HIF- 2α in modulating β-catenin activation of AURKA and formation of primary cilia [89].

Loss of VHL and induction of HIF-1α regulate HEF1/ NEDD9 levels [71, 90]. Although we observed an increase in HEF1 expression in cells that have lost VHL, stabilized HIF-1α inhibited HEF1, similar to that observed with AURKA. A recent report identified HEF1 as a novel target of Wnt signaling providing a potential mechanism by which HIF-1α modulates HEF1 [91]. These data suggest that HIF-1α inhibits both AURKA and HEF1 via β-catenin–driven transcription. AURKA is a direct target of Wnt/β-catenin in multiple myeloma, and was reported to stabilize β-catenin by binding Axin and preventing its association with GSK3β to form the β-catenin destruction complex in glioma-initiating cells [77, 92]. Phosphorylation of β-catenin by casein kinase 1 (CK1) and GSK3β targets it for degradation, and GSK3β phosphorylation at Ser9 inhibits GSK3β's kinase activity in gastric cancer [92]. We show increased phosphorylation of GSK3β (S9) in cells that have elevated AURKA resulting from loss of VHL, highlighting a crucial positive feedback loop by which AURKA potentiates its own expression via activation of β-catenin. A recent report

showed a requirement for the combined inactivation of GSK3β and VHL in destabilizing the ciliary microtubules [12]. Although loss of VHL alone was sufficient to exacerbate AURKA and promote loss of primary cilia in our studies, elevated AURKA inactivated GSK3β, confirming inactivation of both proteins in driving ciliary abnormalities in our model. Given the critical role AURKA plays in regulating primary cilia, its enhanced expression resulting from activation of β-catenin provides us with a potential target that can be modulated to abrogate the ciliary defects associated with VHL disease [14]. Current efforts identifying small molecule inhibitors of β-catenin have generated several promising molecules, including iCRT14, specific in inhibiting catenin responsive transcription, without any effect on β-catenin degradation or β-catenin interactions with junction proteins [80, 93]. Deregulation of Wnt/β-catenin signaling was recently reported in several other ciliopathies in which loss of cystoproteins such as Jouberin, Meckel–Gruber syndrome and nephrocystin are linked to cilia defects as well as nuclear localization and activation of β-catenin transcription [5, 94-96]. Our studies showing elevated AURKA via β-catenin activation in VHL suggest a common pathway driving the renal manifestations associated with ciliopathies. Importantly, our in vitro results showing rescue of the ciliary defect with an inhibitor of β-catenin are promising and warrant further investigation in in vivo models, and perhaps other disease settings.

METHODS AND MATERIALS

Cell Culture

RCC cell lines (Caki-1, 786-O, ACHN, 769-P, and A-498; ATCC) were maintained in McCoy's 5Amedia (Caki-1), RPMI-1640media (786-O), or MEM media

(ACHN, 769-P, and A-498) supplemented with 10% FBS (Sigma-Aldrich, St. Louis, MO). hTERT RPE-1 cells (a kind gift from Dr. Gregory Pazour, University of Massachusetts Medical School) were maintained in DMEM/F-12 media (Life Technologies, Carlsbad, CA), supplemented with 10% FBS. All cells were maintained in 5% CO2 at 37°C, and experiments were performed in fully confluent cultures, starved (serum-free media) for 48 hours to promote ciliogenesis. All human cell lines were validated using the Characterized Cell Line Core Facility (University of Texas MD Anderson Cancer Center).

Constructs, Transfections, and Treatments

Human β-catenin construct (plasmid 16828) was purchased from Addgene, and transfected into hTERT RPE-1 cells using Lipofectamine2000 (Invitrogen) according to the manufacturer's instructions. On-Target plus SMART pool siRNAs (non-targeting, VHL-specific siRNA, HIF-1α–specific siRNA, β-catenin–specific siRNA, and TCF-1–specific siRNA) were transfected into cells using DharmaFECT1 (Thermo Fisher Scientific, Pittsburgh, PA), per the manufacturer's recommendations. Dimethyloxalylglycine (1 mM) and defroxamine (250 μM) (Sigma- Aldrich) were solubilized in water; cells were simultaneously treated, and were starved 6–8 hours after transfections for 48 hours. iCRT14 (Tocris Bioscience, Bristol, UK) was resuspended in ethanol, and cells were treated at a final concentration of 15 μM with serum starvation for 48 hours.

Cell Lysates and Antibodies

Cell lysates were collected in cold 13cell lysis buffer (20 mM Tris [pH 7.5], 150 mM NaCl, 1 mM EDTA, 1mMEGTA, 1% Triton X-100, 2.5 mM sodium pyrophosphate) containing 13 Complete protease inhibitor (Roche, Mannheim, Germany) and 1mMNa3VO4. The lysates were analyzed by immunoblotting with the following primary antibodies: anti-AURKA (1:1000), anti-HDAC6 (1:1000), anti-HEF1/ NEDD9 (1:500), anti–phospho-GSK3β (1:1000), anti-GSK3β (1:1000), anti-CyclinD1 (1:1000), anti-VHL (1:500), anti-lactate dehydrogenase (1:1000), and anti-TCF1 (1:1000) from Cell Signaling Technologies (Danvers, CA); anti–c-myc (1:1000), anti–glyceraldehyde-3-phosphate (GAPDH) (1:20,000), and anti-Lamin A/C (1:1000) from Santa Cruz Biotechnology (Santa Cruz, CA); anti–β-catenin (1:2000) and anti–HIF-1α (1:1000) from BD Biosciences (San Jose, CA); anti-active-β-catenin (1:2000) from EMD Millipore (Billerica, MA); and anti-glucose transporter 1 (1:2500) from Abcam, Inc. (Cambridge, MA). Horseradish peroxidase–conjugated goat anti-mouse, goat anti-rabbit, and donkey anti-goat secondary antibodies were purchased from Santa Cruz Biotechnology. Immunoblots were visualized using LumiGLO (KPL, Gaithersburg, MD), Pierce ECL (Thermo Fisher Scientific, Rockford, IL), or Amersham ECL Prime (GE Life Sciences, Pittsburg, PA) substrates.

RT-PCR Analyses

mRNA was isolated from cells using the RNeasy Mini Kit (Qiagen, Valencia, CA), according to the manufacturer's protocol. After RNA extraction, cDNA was prepared by reverse-transcribing 1 μg of RNA using the Invitrogen Superscript First-

Strand Synthesis System for RT-PCR (Invitrogen, Carlsbad, CA). Real-time PCR was performed using the ABI ViiA7 Real-Time PCR system from Applied Biosystems (Foster City, CA). Fast Real-Time TaqMan assays from ABI were used to analyze gene expression of *VHL, AURKA, HIF-1β, CyclinD1*, and *c-myc*. All real-time PCR reactions were performed by mixing Universal Fast Real-Time Master Mix from ABI together with the gene assay mix first and then adding 2 μl of cDNA from each sample to make up a 25-μl volume. GAPDH was used as an endogenous control, which included probe and forward and reverse primers in a 25-μl reaction volume. The following set of conditions were used for each real-time reaction: 95°C for 20 minutes followed by 40 cycles of 1 second at 95°C and 20 seconds at 60°C. The real-time PCR reactions were all performed in triplicate and were quantified using the 2ΔΔ cycle threshold (C_T) method, which uses the average C_T of the GAPDH subtracted from the target gene C_T to obtain the average ΔC_T. The siRNA/mock controls were used as calibrators from which we subtracted individual VHL, AURKA, HIF-1α, CyclinD1, or c-myc siRNA ΔC_T values to obtain the $2\Delta\Delta C_T$. The fold change for the sample was calculated in comparison with the calibrator by taking $22\Delta\Delta C_T$.

Subcellular Fractionation

Cells were harvested, washed with ice-cold PBS, and resuspended in hypotonic buffer (10 mM HEPES [pH 7.2], 10 mM KCl, 1.5 mM MgCl2, 0.1 mM EGTA, 20 mM NaF, 100 μM Na3VO4). After disruption using a Dounce homogenizer, crude nuclei were pelleted by centrifugation and the supernatant was collected as the cytoplasmic fraction. The crude nuclei were resuspended in hypotonic buffer and any unbroken cells

disrupted in the Dounce homogenizer. The pellet after centrifugation at 3000 rpm at 4°C for 5 minutes was washed with a wash buffer (10 mM Tris [pH 7.4], 0.1% NP-40, 0.05% Na-deoxycholate, 10 mM NaCl, 3 mM MgCl2), and lysed in a high-salt buffer (20 mM HEPES [pH 7.4], 0.5 M NaCl, 0.5% NP-40, 1.5 mMMgCl2). The purified nuclear fraction was collected after centrifugation at 14,000 rpm at 4°C for 10 minutes. The nuclear, cytosolic, and membrane fractions were subsequently subjected to SDS-PAGE and immunoblot analysis.

ChIP Assays

hTERT RPE-1 cells were transfected with a β-catenin overexpression construct or a mock control. After serum starvation for 48 hours, the protein-DNA complexes were cross-linked with 1% formaldehyde for 10 minutes. The cells were lysed, and the cell lysate was subsequently sonicated to shear the DNA. Then, 600 μg of DNA from each group was collected. To reduce nonspecific background, the cell lysate was first incubated with agarose beads and salmon sperm DNA. The supernatant was collected, and 20 μl of it was saved to analyze as the initial input for the reaction. The remaining lysate was incubated overnight with 2 μg of the anti–β-catenin or IgG antibody. The protocol provided with the ChIP kit (Upstate Biotechnology) was followed for immunoprecipitation, elution, and reverse cross-linking of the protein-DNA complex. The eluted DNA was purified with the PCR purification kit (Qiagen). Both the eluted and input products were then subjected to PCR analysis using the same previously published primer sets.

Immunofluorescence Analyses

For immunofluorescence staining, hTERT RPE-1 cells were plated on glass coverslips, transfected, and starved 6 hours after transfection for 48 hours to promote ciliogenesis. Cells were fixed in 4% paraformaldehyde for 10 minutes at room temperature, after washes in 1XPBS. We used 0.05% Triton-X to permeabilize the cells, followed by blocking in 3.75% BSA solution for 1 hour at room temperature. Primary antibodies for a-acetylated tubulin (clone 6-11B-1, 1:5000; Sigma-Aldrich) and pericentrin (1:5000; Abcam, Inc.) or β-catenin (1:100; Santa Cruz Biotechnology) in blocking buffer were applied for 1 hour, followed by AlexaFluor 488 and 546 goat anti-mouse or anti-rabbit secondary antibodies (Life Technologies) for another hour. Cells were counterstained with 49, 6-diamidino-2-phenylindole (Life Technologies) and mounted using ProLong Gold antifade reagent (Life Technologies). Cells were visualized using a Deltavision deconvolution microscope (Applied Precision) at X60 magnification. Images were analyzed using Imaris software (Bitplane). All experiments were performed in three independent replicates unless otherwise specified, and image analyses performed on at least 100 individual cells from each replicate.

Statistical Analyses

All statistical analyses were performed using the t test (one-tailed) for determination of differences between the average values of quantitation data obtained from densitometric analyses of immunoblots and average values obtained from RT-PCR analyses. The SEM was calculated and P values of P, 0.01 and P, 0.05 were considered statistically significant.

CHAPTER III

ESTABLISHING A RELATIONSHIP BETWEEN PRIMARY CILIA AND COLON CANCER

INTRODUCTION

The adenomatous polyposis coli (*APC*) gene, frequently mutated in colorectal cancers, often causes familial adenomatous polyposis (FAP) arising from germline mutations. Gardner's syndrome, a subtype of FAP, produces phenotypic characteristics similar to those seen in many ciliopathies [47, 97]. This connection brings into question the relationship between APC and primary cilia. It is known that APC sends out a cascade of signals, leading to the proteasomal degradation of β-catenin [29-31, 98]. Overexpression of β-catenin has been linked to several ciliopathies, one of the major being polycystic kidney disease (PKD) leading to cyst and tumor formation in the kidneys [99]. APC has also been shown to stabilize microtubules in vivo and in vitro. It was observed that APC, chaperoned by end binding protein 1 (EB1), localizes to the distal tips of microtubules [100]. Additionally, Dere et al. 2014 has shown that, in VHL null cells that lack primary cilia, β-catenin transcriptionally regulates aurora kinase A (AURKA), which in turn activates histone deacetylase 6 (HDAC6) whose role is to deacetylate α-tubulin and destabilize the primary cilium [101]. The last piece of evidence linking APC and primary cilia is from a publication showing that APC binds to KIF3A, a major ciliary protein [102]. Therefore, we hypothesized that when APC is mutated or lost, primary cilia are not stable and resorb, contributing to tumorigenesis.

Furthermore, we hypothesized that HDAC6 has an opposing effect, contributing to primary cilia destabilization in colon cancer cells, similar to that seen in the kidney, and inhibition of HDAC6 can rescue the ciliary defect.

RESULTS

AURKA signaling is increased in colorectal cancer cell lines

As reported in Dere et al. 2014, AURKA and HDAC6 signaling are increased in cell lines with ciliary loss, and another study showed AURKA interacts with HEF1, activating HDAC6 [14, 101]. These reports led us to hypothesize that CRC cells lose their primary cilia, and that this ciliary loss is due to the same upregulation of proteins seen in previous reports as shown by the schematic in figure 11A. As shown in figure 11B (representative experiment), AURKA, HDAC6 and β-catenin protein levels were higher in CRC (HCT116, SW48, SW480, CaCo2) cells compared with non-transformed (hTERT RPE-1, CCD841) cells. Using human retinal pigmented epithelial (hTERT RPE-1) cells, a well characterized model of ciliogenesis, we confirmed that our non-transformed colon (CCD841) cells produced primary cilia and the CRC cells produced little (white arrows) or no primary cilia (Figure 10C).

HDAC6 inhibition by Tubacin in SW480 CRC cells rescues primary cilia

To further explore the role of HDAC6 in ciliogenesis in colon cancer we inhibited the ability of HDAC6 to deacetylate its targets (without HDAC6 turnover) using a pharmacologic inhibitor, Tubacin. We treated a variety of our normal and CRC cell lines with Tubacin (2 μM and 5 μM) and confirmed that HDAC6 total levels were

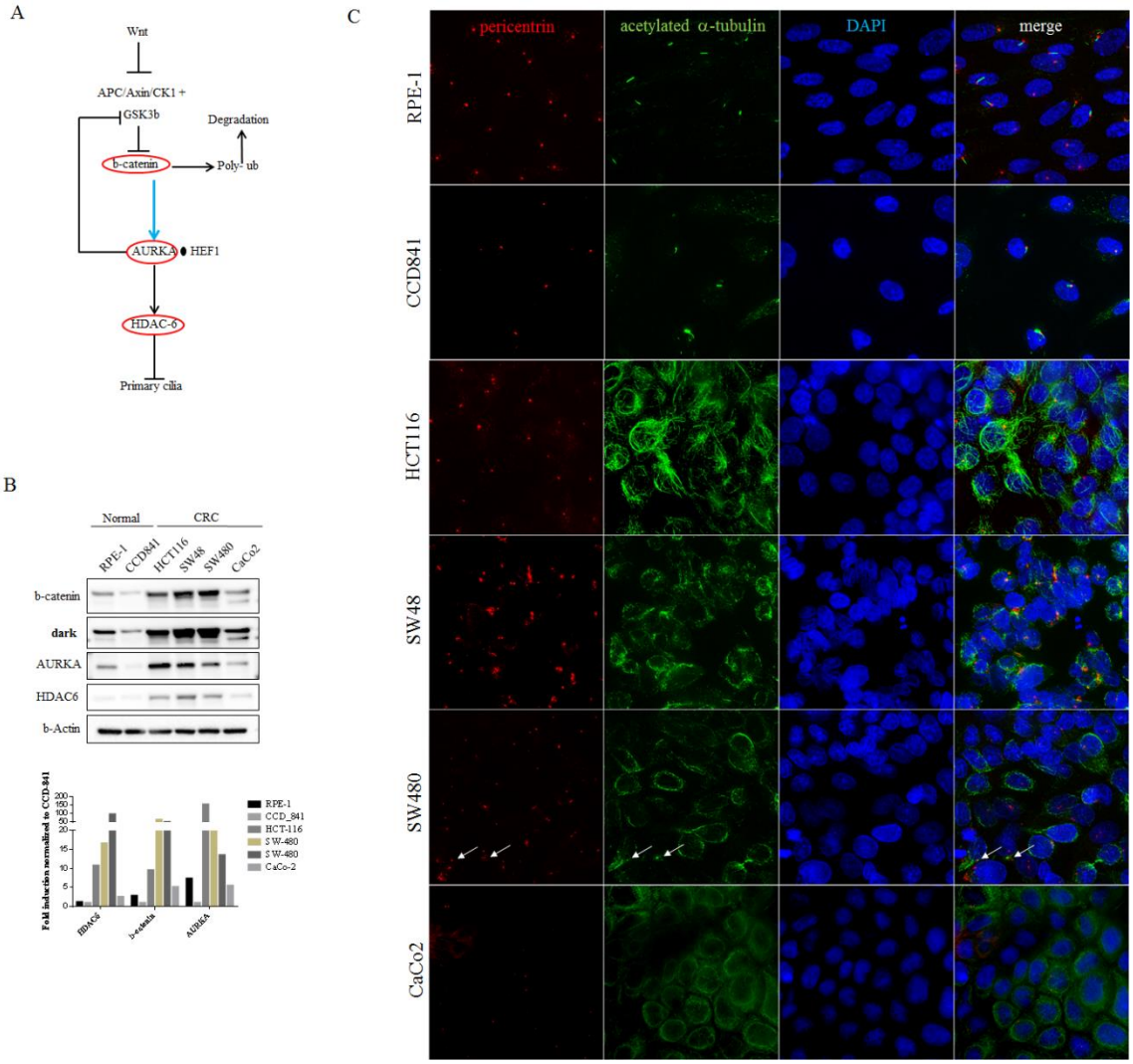

Figure 11. HDAC6 ciliary resorption pathway is increased in CRC. (A) Schematic of ciliogenesis pathway proteins. (B) Lysates from normal or CRC cells are immunoblotted with the indicated antibodies (top) and quantified using densitometric analysis of protein expression normalized to β-actin. Analysis plotted as a graph (bottom) showing increased HDAC6, β-catenin and AURKA protein expression in CRC (HCT116, SW48, SW480, CaCo2) cells compared to normal (hTERT RPE-1, CCD841) cells. (C) Immunofluorescence staining of normal (hTERT RPE-1, CCD841) cells and CRC (HCT116, SW48, SW480, CaCo2) cells serum starved for 48 hours, using pericentrin (basal body marker, red) and acetylated α-tubulin (cilia marker, green). DAPI (blue) was used as a counterstain for the nuclei.

not changing but its ability to deacetylate was inhibited, looking at acetylated α-tubulin levels, which were increased in all cell lines (Figure 12A), including the SW480 cell line

(Figure 12C) when treated with Tubacin. Due to the increase of acetylated α-tubulin levels, staining with the acetylated α-tubulin antibody overexposed the microtubules (also made up of α-tubulin, β-tubulin dimers) and the primary cilia could not be visualized. Therefore, when treating cells with Tubacin we used an alternate ciliary marker, ADP ribosylation factor 13b (ARL13b) and confirmed through staining that this antibody localized to primary cilia (Figure 12B). With this staining we also confirmed the loss of primary cilia in CRC cells. These data led us to hypothesize that primary cilia loss in CRC cells can be rescued with treatment of Tubacin, inhibiting HDAC6 allowing for the acetylation and stabilization of primary cilia. Thus, we treated SW480 CRC cells with Tubacin (2 μM) and observed a dramatic increase in the number of cells that produced primary cilia (Figure 12D), as shown by the white arrows.

Knockdown of APC cells shortens primary cilia

In the majority of CRC cases, inactivating APC or activating β-catenin mutations lead to β-catenin accumulation which we observed in our CRC cells lines compared to non-transformed [30]. Recent reports indicate that β-catenin transcriptionally activates AURKA, leading to ciliary resorption [101]. Additionally, it has been reported that APC localizes to and moves along microtubules via end-binding protein 1 (EB1) and the kinesin superfamily (KIF) [100, 102]. Therefore, we hypothesized that APC is involved in ciliogenesis. To explore the involvement of APC, we used small interfering RNA (siRNA) to knock down APC in our non-transformed (hTERT RPE1, CCD841) cells. RT-PCR analysis showed a 60% and 81% efficiency of knockdown, respectively, in

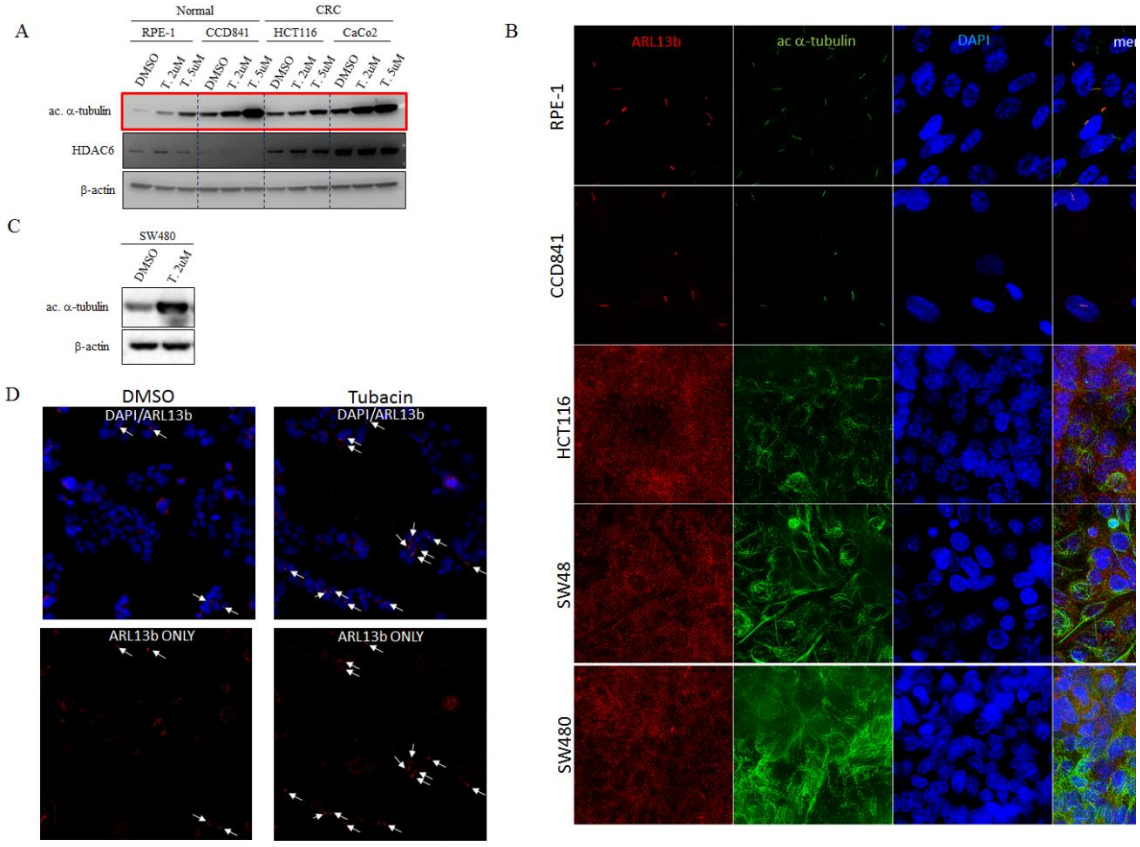

Figure 12. Tubacin treatment in SW480 CRC cells rescues primary cilia. (A) Normal and CRC cells were treated with vehicle (DMSO) or Tubacin (2uM, 5μM) and are immunoblotted with the indicated antibodies, β-actin is used as an internal control. (B) Immunofluorescence staining of normal (hTERT RPE-1, CCD841) cells and CRC (HCT116, SW48, SW480) cells serum starved for 48 hours, using ARL1b (primary cilia marker, red) and acetylated α-tubulin (cilia marker, green). DAPI (blue) was used as a counterstain for the nuclei. (C) SW480 CRC cells were treated with vehicle (DMSO) or Tubacin 2μM and are immunoblotted with the acetylated α-tubulin antibody, β-actin is used as an internal control. (D) Immunofluorescence staining of SW480 CRC cells treated with vehicle (DMSO) or Tubacin 2μM and serum starved for 48 hours, using ARL1b (primary cilia marker, red). DAPI (blue) was used as a counterstain for the nuclei.

cells expressing APC-specific siRNA compared with scrambled control (Figure 13A, Figure 14A). Since no APC antibody could be validated for western analysis, a total β-catenin antibody was used as an indirect output for APC knockdown, which we confirmed in both the hTERT RPE-1 and CCD841 non-transformed cell lines, showing

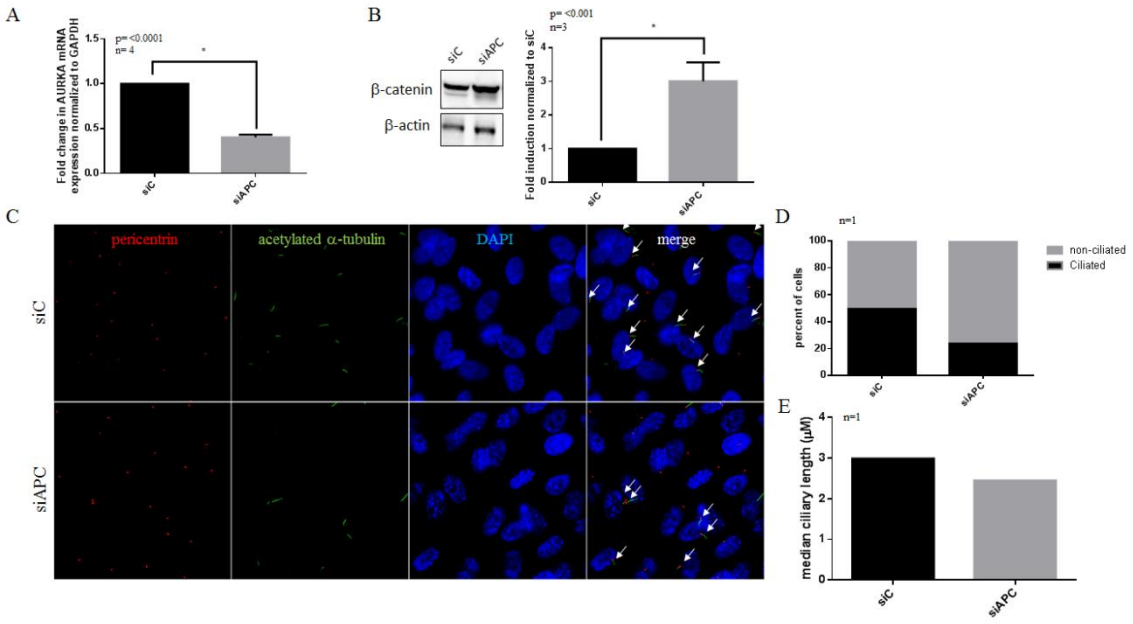

Figure 13. APC knockdown in hTERT RPE-1 cells results in primary cilia shortening. (A) RT-PCR analyses of hTERT RPE-1 cells expressing siC (scrambled) or siAPC showing APC mRNA transcript levels as indicated (p<0.001). (B) Immunoblot analyses from hTERT RPE-1 cells transfected with either siC or siAPC probed with total β-catenin and b-actin. The graph represents the densitometric analyses from three independent replicates showing protein expression normalized to b-actin (loading control) (p<0.001). (C) Immunofluorescence staining of hTERT RPE-1 cells expressing siC or siAPC, using pericentrin (basal body marker, red) and acetylated α-tubulin (cilia marker, green). The nuclei are counterstained with DAPI (blue). The white arrows show the primary cilia. (D) Immunofluorescence images were analyzed using FIJI software to quantitate the number of cells containing (black bars) or not containing (grey bars) primary cilia from >300 individual hTERT RPE-1 cells transfected with siC or siAPC. A representative experiment is shown. (E) Immunofluorescence images were analyzed using FIJI software to measure the length of the primary cilia from >300 individual hTERT RPE-1 cells transfected with siC (black bars) or siAPC (grey bars). A representative experiment is shown. *Statistically significant differences.

increased total β-catenin levels when treated with siAPC (Figure 13B, Figure 14B). We found that knocking down APC revealed a decrease in the number of cells that could generate a primary cilium (Figure 13C, Figure 14C). Quantitative analysis revealed a significant decrease in the percent of cells that could produce a primary cilium (Figure 13D, Figure 14D). In the cells that retained their primary cilium, we saw a significant

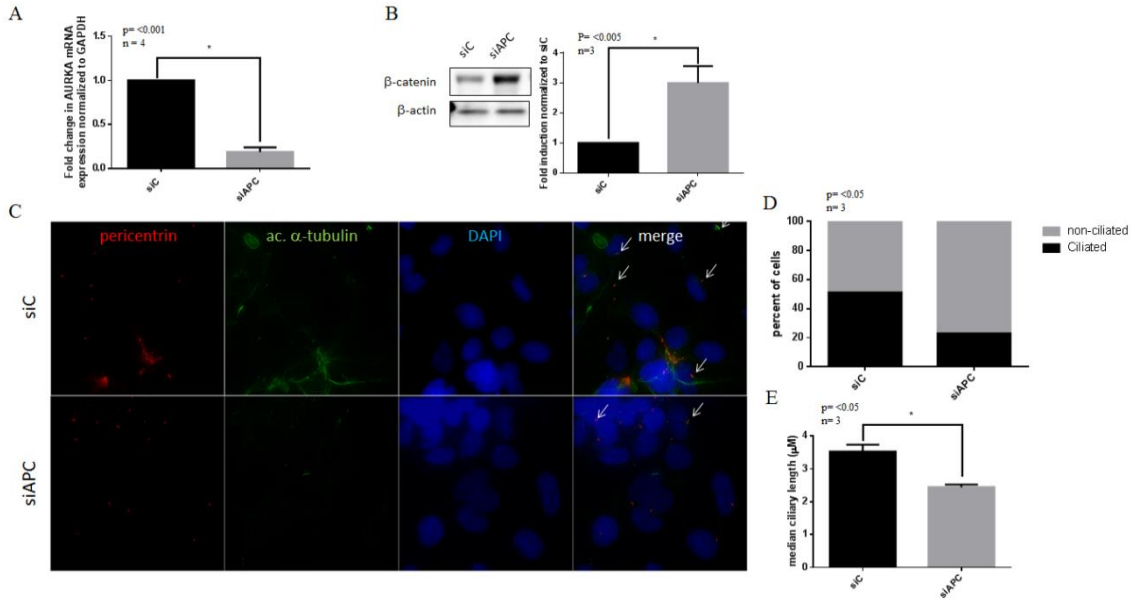

Figure 14. APC knockdown in CCD841 cells results in primary cilia shortening. (A) RT-PCR analyses of CCD841 cells expressing siC (scrambled) or siAPC showing APC mRNA transcript levels as indicated ($p<0.001$). (B) Immunoblot analyses from CCD841 cells transfected with either siC or siAPC probed with total β-catenin and b-actin. The graph represents the densitometric analyses from three independent replicates showing protein expression normalized to b-actin (loading control) ($p<0.005$). (C) Immunofluorescence staining of CCD841 cells expressing siC or siAPC, using pericentrin (basal body marker, red) and acetylated *α*-tubulin (cilia marker, green). The nuclei are counterstained with DAPI (blue). The white arrows show the primary cilia. (D) Immunofluorescence images were analyzed using FIJI software to quantitate the number of cells containing (black bars) or not containing (grey bars) primary cilia from >300 individual CCD841 cells transfected with siC or siAPC. ($p<0.05$) (E) Immunofluorescence images were analyzed using FIJI software to measure the length of the primary cilia from >300 individual CCD841 cells transfected with siC (black bars) or siAPC (grey bars). *Statistically significant differences ($p<0.05$).

shortening (Figure 13E, Figure 14E). Notably, not all cells in the population successfully took up the siRNA, explaining the moderate estimates.

DISCUSSION

APC is an important tumor suppressor gene that contributes to cell homeostasis via β-catenin degradation. Dysfunction of *APC* contributes to CRC, FAP and Gardner's Syndrome, the latter exhibiting extracolonic manifestations, similar to those seen in

many ciliopathies, including CHRPE, renal cysts and fibrosis [47]. Along with the ciliary phenotypes seen in individuals with APC mutations, reports have shown APC localizing to the growing end of microtubules aiding in their stabilization [100, 103, 104]. Our results link APC to primary cilia in non-transformed epithelial cells. We show that knockdown of APC in our non-transformed epithelial cells inhibits primary cilia formation. However, the exact mechanisms are still unknown. Given the previous data APC could regulate primary cilia stability through direct binding. Hence, when APC is mutated it can no longer bind to the primary cilia, leading to destabilization and resorption. Song et al. 2014 observed loss of primary cilia when APC truncation mutations at the N-terminal were made, however, it was proposed that the PI3K/AKT pathway was responsible for inhibiting GSK3β, causing a positive feedback loop with β-catenin [48].

Alternatively, APC could play an indirect role in ciliary stability through negative regulation of β-catenin. As a result of APC loss, β-catenin would accumulate, contributing to AURKA overexpression. β-Catenin was previously shown to transcriptionally activate AURKA expression, subsequently activating HDAC6 causing ciliary resorption [101]. Or results corroborate this pathway regulation, showing increased AURKA, HDAC6 and β-catenin expression in CRC cells, correlating with a reduction of primary cilia. Given HDAC6's ability to deacetylate and destabilize the primary cilium, it has become an attractive target that can be regulated to prevent ciliary defects associated with β-catenin accumulation in CRC patients. Currently, there are numerous pan HDAC inhibitors but few HDAC6 specific inhibitors. Tubacin, a HDAC6

specific inhibitor, binds to the second deacetylase domain on HADC6, inhibiting its ability to deacetylate its binding partners. We show that inhibition of HDAC6 via Tubacin in SW480 CRC cells restores the ciliary defect. This data warrants further investigation into inhibitors of the ciliary pathway, such as AURKA and β-catenin inhibitors, to restore ciliary defect in patients with inactivating APC or activating β-catenin mutations.

METHODS AND MATERIALS

Cell Culture

Colon cell lines were maintained in McCoy's 5A medium (1x) + L-glutamine (HCT116, SW480) (Life Technologies, Carlsbad, CA), Eagle's Minimum Essential Medium + L-glutamine (CCD841) (ATCC, Manassas, VA) or Leibovitz's L-15 Medium + L-glutamine (SW48), supplemented with 10% FBS (Atlanta Biologicals, Flowery Branch, GA) and 1% Penicillin-Streptomycin (Life Technologies, Carlsbad, CA). The CaCo2 colon cancer cell line was maintained in Eagle's Minimum Essential Medium + L-glutamine (ATCC, Manassas, VA) supplemented with 20% FBS (Atlanta Biologicals, Flowery Branch, GA) and 1% Pen-Strep (Life Technologies, Carlsbad, CA). hTERT RPE-1 cells (a kind gift from Dr. Cheryl Walker, Texas A&M University Health Science Center, Institute of Biosciences and Technology) were maintained in DMEM/F-12 media (Life Technologies, Carlsbad, CA), supplemented with 10% FBS (Atlanta Biologicals, Flowery Branch, GA) and 1% Pen-Strep (Life Technologies, Carlsbad, CA). All cells were maintained in 5% CO2 at 37°C, and experiments were performed in fully

confluent cultures, starved starved (FBS-free media) for 48 hours to promote ciliogenesis.

Transfections, and Treatments

On-Target plus SMART pool siRNAs (non-targeting and APC-specific siRNA) were transfected into cells using RNAimax (Thermo Fisher Scientific, Pittsburgh, PA), per the manufacturer's recommendations. Tubacin (5 μM) (Sigma-Aldrich, St. Louis, MO) was solubilized in DMSO; cells were simultaneously treated and serum starved with transfections for 48 hours.

Cell Lysates and Antibodies

Cell lysates were collected in cold 1x cell lysis buffer (20 mM Tris [pH 7.5], 150 mM NaCl, 1 mM EDTA, 1mM EGTA, 1% Triton X-100, 2.5 mM sodium pyrophosphate, 1 mM beta-glycerophosphate, 1mM Na3VO4, 1μg/mL Leupeptin) containing Complete protease inhibitor (Roche, Mannheim, Germany). The lysates were analyzed by immunoblotting with the following primary antibodies: anti-AURKA [C3] (1:1000) from GeneTex (Irvine, CA), anti-HDAC6 [D21B10] (1:1000) and anti–β-catenin (1:1000) from Cell Signaling Technologies (Danvers, CA), anti-HDAC6 [EPR1698(2] (1:1000) from Abcam, Inc. (Cambridge, MA), anti-β-actin [clone AC-15] (1:5000) or (1:20000) from Sigma-Aldrich (Dt. Louis, MO). Horseradish peroxidase–conjugated goat anti-mouse and goat anti-rabbit secondary antibodies were purchased from Bio-Rad (Hercules, CA). Immunoblots were visualized using Western Lightning Plus-ECL substrates from Perkin-Elmer (Waltham, MA).

RT-PCR Analyses

mRNA was isolated from cells using the RNeasy Mini Kit (Qiagen, Valencia, CA), according to the manufacturer's protocol. After RNA extraction, cDNA was prepared by reverse-transcribing 1 μg of RNA using the Invitrogen Superscript First-Strand Synthesis System for RT-PCR (Invitrogen, Carlsbad, CA). Real-time PCR was performed using the Roche lightcycler 96 from Roche (Basel, Switzerland). SybrGreen assays from Roche were used to analyze gene expression of APC. All real-time PCR reactions were performed by mixing FastStart Essential DNA Green Master Mix from Roche together with the gene assay primer mix first and then adding 2 μl of cDNA from each sample to make up a 10-μl volume. GAPDH was used as an endogenous control, which included probe and forward and reverse primers in a 10-μl reaction volume. The following set of conditions were used for each real-time reaction: 95°C for 10 minutes followed by 45 cycles of 10 seconds at 95°C, 10 seconds at 60°C, 10 seconds at 75°C. Melt curves were added to the real-time reaction: 10 seconds at 95°C, 60 seconds at 65°C, 1 second at 97°C. The real-time PCR reactions were all performed in triplicate and were quantified using the delta delta cycle threshold ($\Delta\Delta C_T$) method, which uses the average C_T of the GAPDH subtracted from the average C_T of target gene to obtain the ΔC_T. The siRNA controls were used as calibrators from which we subtracted individual APC siRNA ΔC_T values to obtain the $\Delta\Delta C_T$. The fold change for the sample was calculated in comparison with the calibrator by taking $2^{\wedge -\Delta\Delta C_T}$.

Immunofluorescence Analyses

For immunofluorescence staining, all cells were plated on poly-d-lysine treated glass coverslips, transfected or treated, and starved for 48 hours to promote ciliogenesis. Cells were fixed in 4% paraformaldehyde for 30 minutes on ice, after washes in 1X PBS. We used 0.05% Triton-X to permeabilize the cells, rocking for 30 minutes, followed by blocking in 5% BSA solution for 1 hour at room temperature or 0.01% triton-X in blocking solution for 1 hour at room temperature. Primary antibodies for anti-acetylated α-tubulin (clone 6-11B-1, 1:4000; Santa Cruz Biotechnology), anti-pericentrin (1:4000; Abcam, Inc.), or anti-ARL13b (1:4000; Protein Tech) in blocking buffer were applied overnight with ice or 1 hour at 37C, followed by 5-10 minute washes in PBS plus calcium and magnesium (PBS++) followed by AlexaFluor 488 donkey anti-mouse IgG (H+L), Alexafluor 647 donkey anti-rabbit IgG (H+L), Alexafluor 488 goat anti-mouse IgG_{2b} (γ2b), or Alexafluor 546 goat anti-mouse IgG_1 (γ1) secondary antibodies (Life Technologies) for one hour followed by 5-10 minute washes in PBS++. Cells were post-fixed in 4% paraformaldehyde for 10 minutes, washed 1 time in PBS++ then counterstained with 4', 6-diamidino-2-phenylindole (DAPI) (Life Technologies) and mounted using SlowFade® Gold Antifade Reagent (Life Technologies). Cells were visualized using a DeltaVision Elite deconvolution microscope (Applied Precision) using a 60x na= 1.42 oil objective, or 20x na= 0.45 dry objective. Images were analyzed using Image J or FIJI software (NIH). All experiments were performed in three independent replicates unless otherwise specified, and image analyses performed on at least 300 individual cells from each replicate.

Statistical Analyses

All statistical analyses were performed using the t test (one-tailed) for determination of differences between the average values of quantitation data obtained from densitometric analyses of immunoblots and average values obtained from RT-PCR analyses. The SEM was calculated and P values of $P < 0.01$ and $P < 0.05$ were considered statistically significant.

CHAPTER IV

SUMMARY AND CONCLUSIONS

CONCLUSIONS

These studies dissected the roles that β-catenin plays in ciliogenesis. Primary cilia resorption is associated with VHL loss in ccRCC patients and these ciliary defects often lead to renal cysts and tumors [49, 60, 61]. Studies have indicated elevated levels AURKA are associated with ciliary loss, however the exact mechanisms linking AURKA to primary cilia are unknown in the settings of ccRCC or CRC [50, 51, 81, 82]. In our studies, we have shown links between β-catenin and AURKA overexpression associating with ciliary resorption during VHL loss. Additionally, when β-catenin is inhibited, loss of AURKA expression is observed, accompanied by rescued ciliogenesis. Although HIF-1 was previously reported to positively regulate AURKA, our data illustrate an inhibitory role in normal and VHL-proficient RCC cell lines, possibly due to HIF-1α playing a role as a competitive inhibitor to β-catenin responsive transcription, sequestering β-catenin away from TCF4 to prevent activation of its downstream targets [71, 76, 83, 84].

Previous studies have shown that induction of HIF-1α via VHL loss leads to increased HEF1 expression levels [71, 90]. We confirmed the VHL results, observing an increase in HEF1 expression during VHL knockdown, however HIF-1α accumulation resulted in decreased HEF1 expression, analogous with the expression levels of AURKA. Dutta-Simmons et al. 2009 showed that AURKA is a direct target of β-

catenin-driven transcription and Li et al. 2011 reported HEF1 as another target of Wnt signaling, which suggests that HIF-1α could be modulating both ciliary proteins through β-catenin [77, 91]. Furthermore, GSK3β, a crucial part of the β-catenin destruction complex can be inhibited via phosphorylation at Ser9 by AURKA, indicating a positive feedback loop [79]. We illustrated this point by knocking down VHL, revealing increases in GSK3β expression similar to AURKA expression. Correspondingly, in CRC, APC loss leads to β-catenin accumulation, which we show contributes to AURKA overexpression. Or results in CRC cells corroborate the ciliary regulation seen in VHL null cells, showing increased AURKA, HDAC6 and β-catenin expression, correlating with a reduction of primary cilia. However, Song et al. 2014 proposed that the PI3K/AKT pathway was responsible for inhibiting GSK3β, causing a positive feedback loop with β-catenin when APC acquired N-terminal truncation mutations [48].

β-catenin offers itself as a potential therapeutic target to repress the ciliary defect seen in both VHL disease and CRC, due to the significant role it plays in ciliary regulation, triggering AURKA and HDAC6 activation. Identification of small molecule inhibitors of β-catenin has yielded iCRT14, an inhibitor of β-catenin responsive transcription that could be useful in many ciliopathies showing dysfunction of Wnt/ β-catenin signaling, including Gardner's Syndrome, Joubert Syndrome, familial adenomatous polyposis (FAP), and Meckel-Gruber syndrome [47, 94, 96, 105]. Our in vitro studies have shown that iCRT14, a β-catenin inhibitor, rescues the ciliary defect as seen in our VHL-null cells. We have also illustrated the importance of HDAC6 in ciliary

destabilization. Our results show that treatment of SW480 CRC cells with Tubacin, a well-known HDAC6 inhibitor that blocks its ability to deacetylate, rescues primary cilia, restoring the ciliary defect. Importantly, our studies show rescue of the ciliary defect in both ccRCC and CRC settings with inhibitors of β-catenin and HDAC6 are encouraging and warrant further investigation in vivo models.

REFERENCES

1. Kim, S. and L. Tsiokas, *Cilia and cell cycle re-entry: more than a coincidence.* Cell Cycle, 2011. **10**(16): p. 2683-90.
2. Menco, B.P. and A.I. Farbman, *Genesis of cilia and microvilli of rat nasal epithelia during pre-natal development. II. Olfactory epithelium, a morphometric analysis.* J Cell Sci, 1985. **78**: p. 311-36.
3. Tucker, R.W., A.B. Pardee, and K. Fujiwara, *Centriole ciliation is related to quiescence and DNA synthesis in 3T3 cells.* Cell, 1979. **17**(3): p. 527-35.
4. Gallagher, B.C., *Primary cilia of the corneal endothelium.* Am J Anat, 1980. **159**(4): p. 475-84.
5. Wheatley, D.N., *Primary cilia in normal and pathological tissues.* Pathobiology, 1995. **63**(4): p. 222-38.
6. Moller, P.C., J.P. Chang, and L.R. Partridge, *Immunocytochemical localization of tubulin with colloidal gold in cilia of rabbit tracheal epithelial cultures.* Tissue Cell, 1983. **15**(1): p. 39-45.
7. Barnes, B.G., *Ciliated secretory cells in the pars distalis of the mouse hypophysis.* J Ultrastruct Res, 1961. **5**: p. 453-67.
8. Ishikawa, H. and W.F. Marshall, *Ciliogenesis: building the cell's antenna.* Nat Rev Mol Cell Biol, 2011. **12**(4): p. 222-34.
9. Brooks, E.R. and J.B. Wallingford, *Multiciliated cells.* Curr Biol, 2014. **24**(19): p. R973-82.

10. Rocha, C., et al., *Tubulin glycylases are required for primary cilia, control of cell proliferation and tumor development in colon.* EMBO J, 2014. **33**(19): p. 2247-60.

11. Abou Alaiwi, W.A., S.T. Lo, and S.M. Nauli, *Primary cilia: highly sophisticated biological sensors.* Sensors (Basel), 2009. **9**(9): p. 7003-20.

12. Thoma, C.R., et al., *pVHL and GSK3beta are components of a primary cilium-maintenance signalling network.* Nat Cell Biol, 2007. **9**(5): p. 588-95.

13. Basten, S.G. and R.H. Giles, *Functional aspects of primary cilia in signaling, cell cycle and tumorigenesis.* Cilia, 2013. **2**(1): p. 6.

14. Pugacheva, E.N., et al., *HEF1-dependent Aurora A activation induces disassembly of the primary cilium.* Cell, 2007. **129**(7): p. 1351-63.

15. Engel, B.D., et al., *The role of retrograde intraflagellar transport in flagellar assembly, maintenance, and function.* J Cell Biol, 2012. **199**(1): p. 151-67.

16. Pan, J. and W. Snell, *The primary cilium: keeper of the key to cell division.* Cell, 2007. **129**(7): p. 1255-7.

17. Corbit, K.C., et al., *Vertebrate Smoothened functions at the primary cilium.* Nature, 2005. **437**(7061): p. 1018-21.

18. Rohatgi, R., L. Milenkovic, and M.P. Scott, *Patched1 regulates hedgehog signaling at the primary cilium.* Science, 2007. **317**(5836): p. 372-6.

19. Hirokawa, N., et al., *Kinesin associates with anterogradely transported membranous organelles in vivo.* J Cell Biol, 1991. **114**(2): p. 295-302.

20. Schnapp, B.J., T.S. Reese, and R. Bechtold, *Kinesin is bound with high affinity to squid axon organelles that move to the plus-end of microtubules.* J Cell Biol, 1992. **119**(2): p. 389-99.

21. Johnson, K.A. and J.L. Rosenbaum, *Polarity of flagellar assembly in Chlamydomonas.* J Cell Biol, 1992. **119**(6): p. 1605-11.

22. Piperno, G., K. Mead, and S. Henderson, *Inner dynein arms but not outer dynein arms require the activity of kinesin homologue protein KHP1(FLA10) to reach the distal part of flagella in Chlamydomonas.* J Cell Biol, 1996. **133**(2): p. 371-9.

23. Cole, D.G., et al., *Chlamydomonas kinesin-II-dependent intraflagellar transport (IFT): IFT particles contain proteins required for ciliary assembly in Caenorhabditis elegans sensory neurons.* J Cell Biol, 1998. **141**(4): p. 993-1008.

24. Lin, F., et al., *Kidney-specific inactivation of the KIF3A subunit of kinesin-II inhibits renal ciliogenesis and produces polycystic kidney disease.* Proc Natl Acad Sci U S A, 2003. **100**(9): p. 5286-91.

25. Pazour, G.J., et al., *Chlamydomonas IFT88 and its mouse homologue, polycystic kidney disease gene tg737, are required for assembly of cilia and flagella.* J Cell Biol, 2000. **151**(3): p. 709-18.

26. Lancaster, M.A., J. Schroth, and J.G. Gleeson, *Subcellular spatial regulation of canonical Wnt signalling at the primary cilium.* Nat Cell Biol, 2011. **13**(6): p. 700-7.

27. MacDonald, B.T., K. Tamai, and X. He, *Wnt/beta-catenin signaling: components, mechanisms, and diseases.* Dev Cell, 2009. **17**(1): p. 9-26.

28. Tolwinski, N.S., et al., *Wg/Wnt signal can be transmitted through arrow/LRP5,6 and Axin independently of Zw3/Gsk3beta activity.* Dev Cell, 2003. **4**(3): p. 407-18.

29. Hart, M.J., et al., *Downregulation of beta-catenin by human Axin and its association with the APC tumor suppressor, beta-catenin and GSK3 beta.* Curr Biol, 1998. **8**(10): p. 573-81.

30. Munemitsu, S., et al., *Regulation of intracellular beta-catenin levels by the adenomatous polyposis coli (APC) tumor-suppressor protein.* Proc Natl Acad Sci U S A, 1995. **92**(7): p. 3046-50.

31. Rubinfeld, B., et al., *Binding of GSK3beta to the APC-beta-catenin complex and regulation of complex assembly.* Science, 1996. **272**(5264): p. 1023-6.

32. Tetsu, O. and F. McCormick, *Beta-catenin regulates expression of cyclin D1 in colon carcinoma cells.* Nature, 1999. **398**(6726): p. 422-6.

33. Dejmek, J., et al., *Wnt-5a/Ca2+-induced NFAT activity is counteracted by Wnt-5a/Yes-Cdc42-casein kinase 1alpha signaling in human mammary epithelial cells.* Mol Cell Biol, 2006. **26**(16): p. 6024-36.

34. Gao, B., et al., *Wnt signaling gradients establish planar cell polarity by inducing Vangl2 phosphorylation through Ror2.* Dev Cell, 2011. **20**(2): p. 163-76.

35. Hikasa, H., et al., *The Xenopus receptor tyrosine kinase Xror2 modulates morphogenetic movements of the axial mesoderm and neuroectoderm via Wnt signaling.* Development, 2002. **129**(22): p. 5227-39.

36. Oishi, I., et al., *The receptor tyrosine kinase Ror2 is involved in non-canonical Wnt5a/JNK signalling pathway.* Genes Cells, 2003. **8**(7): p. 645-54.

37. Nauli, S.M., et al., *Polycystins 1 and 2 mediate mechanosensation in the primary cilium of kidney cells.* Nat Genet, 2003. **33**(2): p. 129-37.

38. Nauli, S.M., et al., *Endothelial cilia are fluid shear sensors that regulate calcium signaling and nitric oxide production through polycystin-1.* Circulation, 2008. **117**(9): p. 1161-71.

39. Yoder, B.K., X. Hou, and L.M. Guay-Woodford, *The polycystic kidney disease proteins, polycystin-1, polycystin-2, polaris, and cystin, are co-localized in renal cilia.* J Am Soc Nephrol, 2002. **13**(10): p. 2508-16.

40. Patel, T.P., et al., *Automated quantification of neuronal networks and single-cell calcium dynamics using calcium imaging.* J Neurosci Methods, 2015. **243**: p. 26-38.

41. Luo, Y., et al., *Native polycystin 2 functions as a plasma membrane Ca2+-permeable cation channel in renal epithelia.* Mol Cell Biol, 2003. **23**(7): p. 2600-7.

42. Abdul-Majeed, S. and S.M. Nauli, *Calcium-mediated mechanisms of cystic expansion.* Biochim Biophys Acta, 2011. **1812**(10): p. 1281-90.

43. Yamaguchi, T., et al., *Cyclic AMP activates B-Raf and ERK in cyst epithelial cells from autosomal-dominant polycystic kidneys.* Kidney Int, 2003. **63**(6): p. 1983-94.

44. Ansley, S.J., et al., *Basal body dysfunction is a likely cause of pleiotropic Bardet-Biedl syndrome.* Nature, 2003. **425**(6958): p. 628-33.

45. Cantagrel, V., et al., *Mutations in the cilia gene ARL13B lead to the classical form of Joubert syndrome.* Am J Hum Genet, 2008. **83**(2): p. 170-9.

46. Marszalek, J.R., et al., *Situs inversus and embryonic ciliary morphogenesis defects in mouse mutants lacking the KIF3A subunit of kinesin-II.* Proc Natl Acad Sci U S A, 1999. **96**(9): p. 5043-8.

47. Gomez Garcia, E.B. and N.V. Knoers, *Gardner's syndrome (familial adenomatous polyposis): a cilia-related disorder.* Lancet Oncol, 2009. **10**(7): p. 727-35.

48. Song, L., et al., *N-terminal truncation mutations of adenomatous polyposis coli are associated with primary cilia defects.* Int J Biochem Cell Biol, 2014. **55**: p. 79-86.

49. Bausch, B., et al., *Renal cancer in von Hippel-Lindau disease and related syndromes.* Nat Rev Nephrol, 2013. **9**(9): p. 529-38.

50. Ferchichi, I., et al., *Aurora A overexpression and pVHL reduced expression are correlated with a bad kidney cancer prognosis.* Dis Markers, 2012. **33**(6): p. 333-40.

51. Martin, B., et al., *Identification of pVHL as a novel substrate for Aurora-A in clear cell renal cell carcinoma (ccRCC).* PLoS One, 2013. **8**(6): p. e67071.

52. Stebbins, C.E., W.G. Kaelin, Jr., and N.P. Pavletich, *Structure of the VHL-ElonginC-ElonginB complex: implications for VHL tumor suppressor function.* Science, 1999. **284**(5413): p. 455-61.

53. Lian, X., et al., *Expression and clinical significance of von Hippel-Lindau downstream genes: Jade-1 and beta-catenin related to renal cell carcinoma.* Urology, 2012. **80**(2): p. 485 e7-13.

54. Maxwell, P.H., et al., *The tumour suppressor protein VHL targets hypoxia-inducible factors for oxygen-dependent proteolysis.* Nature, 1999. **399**(6733): p. 271-5.

55. Valladares Ayerbes, M., et al., *Origin of renal cell carcinomas.* Clin Transl Oncol, 2008. **10**(11): p. 697-712.

56. Haase, V.H., *Renal cancer: oxygen meets metabolism.* Exp Cell Res, 2012. **318**(9): p. 1057-67.

57. Li, L. and W.G. Kaelin, Jr., *New insights into the biology of renal cell carcinoma.* Hematol Oncol Clin North Am, 2011. **25**(4): p. 667-86.

58. Thoma, C.R., et al., *Quantitative image analysis identifies pVHL as a key regulator of microtubule dynamic instability.* J Cell Biol, 2010. **190**(6): p. 991-1003.

59. Thoma, C.R., et al., *VHL loss causes spindle misorientation and chromosome instability.* Nat Cell Biol, 2009. **11**(8): p. 994-1001.

60. Pan, J., T. Seeger-Nukpezah, and E.A. Golemis, *The role of the cilium in normal and abnormal cell cycles: emphasis on renal cystic pathologies.* Cell Mol Life Sci, 2013. **70**(11): p. 1849-74.

61. Basten, S.G., et al., *Reduced cilia frequencies in human renal cell carcinomas versus neighboring parenchymal tissue.* Cilia, 2013. **2**(1): p. 2.

62. Kuehn, E.W., G. Walz, and T. Benzing, *Von hippel-lindau: a tumor suppressor links microtubules to ciliogenesis and cancer development.* Cancer Res, 2007. **67**(10): p. 4537-40.

63. Frew, I.J., et al., *pVHL and PTEN tumour suppressor proteins cooperatively suppress kidney cyst formation.* EMBO J, 2008. **27**(12): p. 1747-57.

64. Montani, M., et al., *VHL-gene deletion in single renal tubular epithelial cells and renal tubular cysts: further evidence for a cyst-dependent progression pathway of clear cell renal carcinoma in von Hippel-Lindau disease.* Am J Surg Pathol, 2010. **34**(6): p. 806-15.

65. Ezratty, E.J., et al., *A role for the primary cilium in Notch signaling and epidermal differentiation during skin development.* Cell, 2011. **145**(7): p. 1129-41.

66. Habbig, S., et al., *NPHP4, a cilia-associated protein, negatively regulates the Hippo pathway.* J Cell Biol, 2011. **193**(4): p. 633-42.

67. Schneider, L., et al., *PDGFRalphaalpha signaling is regulated through the primary cilium in fibroblasts.* Curr Biol, 2005. **15**(20): p. 1861-6.

68. Simons, M., et al., *Inversin, the gene product mutated in nephronophthisis type II, functions as a molecular switch between Wnt signaling pathways.* Nat Genet, 2005. **37**(5): p. 537-43.

69. Waters, A.M. and P.L. Beales, *Ciliopathies: an expanding disease spectrum.* Pediatr Nephrol, 2011. **26**(7): p. 1039-56.

70. Ricketts, C., et al., *Analysis of germline variants in CDH1, IGFBP3, MMP1, MMP3, STK15 and VEGF in familial and sporadic renal cell carcinoma.* PLoS One, 2009. **4**(6): p. e6037.

71. Xu, J., et al., *VHL inactivation induces HEF1 and Aurora kinase A.* J Am Soc Nephrol, 2010. **21**(12): p. 2041-6.

72. Chitalia, V.C., et al., *Jade-1 inhibits Wnt signalling by ubiquitylating beta-catenin and mediates Wnt pathway inhibition by pVHL.* Nat Cell Biol, 2008. **10**(10): p. 1208-16.

73. Zhou, M.I., et al., *Tumor suppressor von Hippel-Lindau (VHL) stabilization of Jade-1 protein occurs through plant homeodomains and is VHL mutation dependent.* Cancer Res, 2004. **64**(4): p. 1278-86.

74. Zhou, M.I., et al., *The von Hippel-Lindau tumor suppressor stabilizes novel plant homeodomain protein Jade-1.* J Biol Chem, 2002. **277**(42): p. 39887-98.

75. Shinojima, T., et al., *Renal cancer cells lacking hypoxia inducible factor (HIF)-1alpha expression maintain vascular endothelial growth factor expression through HIF-2alpha.* Carcinogenesis, 2007. **28**(3): p. 529-36.

76. Kaidi, A., A.C. Williams, and C. Paraskeva, *Interaction between beta-catenin and HIF-1 promotes cellular adaptation to hypoxia.* Nat Cell Biol, 2007. **9**(2): p. 210-7.

77. Dutta-Simmons, J., et al., *Aurora kinase A is a target of Wnt/beta-catenin involved in multiple myeloma disease progression.* Blood, 2009. **114**(13): p. 2699-708.

78. Xu, C., N.G. Kim, and B.M. Gumbiner, *Regulation of protein stability by GSK3 mediated phosphorylation.* Cell Cycle, 2009. **8**(24): p. 4032-9.

79. Dar, A.A., A. Belkhiri, and W. El-Rifai, *The aurora kinase A regulates GSK-3beta in gastric cancer cells.* Oncogene, 2009. **28**(6): p. 866-75.

80. Gonsalves, F.C., et al., *An RNAi-based chemical genetic screen identifies three small-molecule inhibitors of the Wnt/wingless signaling pathway.* Proc Natl Acad Sci U S A, 2011. **108**(15): p. 5954-63.

81. Kurahashi, T., et al., *Significance of Aurora-A expression in renal cell carcinoma.* Urol Oncol, 2007. **25**(2): p. 128-33.

82. Maruschke, M., et al., *Expression profiling of metastatic renal cell carcinoma using gene set enrichment analysis.* Int J Urol, 2014. **21**(1): p. 46-51.

83. Cui, S.Y., et al., *The role of Aurora A in hypoxia-inducible factor 1alpha-promoting malignant phenotypes of hepatocelluar carcinoma.* Cell Cycle, 2013. **12**(17): p. 2849-66.

84. Klein, A., D. Flugel, and T. Kietzmann, *Transcriptional regulation of serine/threonine kinase-15 (STK15) expression by hypoxia and HIF-1.* Mol Biol Cell, 2008. **19**(9): p. 3667-75.

85. Fanale, D., et al., *HIF-1 is involved in the negative regulation of AURKA expression in breast cancer cell lines under hypoxic conditions.* Breast Cancer Res Treat, 2013. **140**(3): p. 505-17.

86. Choi, H., et al., *HIF-2alpha enhances beta-catenin/TCF-driven transcription by interacting with beta-catenin.* Cancer Res, 2010. **70**(24): p. 10101-11.

87. Criscimanna, A., et al., *PanIN-specific regulation of Wnt signaling by HIF2alpha during early pancreatic tumorigenesis.* Cancer Res, 2013. **73**(15): p. 4781-90.

88. Park, Y.K., et al., *Hypoxia-inducible factor-2alpha-dependent hypoxic induction of Wnt10b expression in adipogenic cells.* J Biol Chem, 2013. **288**(36): p. 26311-22.

89. Gordan, J.D., et al., *HIF-alpha effects on c-Myc distinguish two subtypes of sporadic VHL-deficient clear cell renal carcinoma.* Cancer Cell, 2008. **14**(6): p. 435-46.

90. Kim, S.H., et al., *Human enhancer of filamentation 1 Is a mediator of hypoxia-inducible factor-1alpha-mediated migration in colorectal carcinoma cells.* Cancer Res, 2010. **70**(10): p. 4054-63.

91. Li, Y., et al., *HEF1, a novel target of Wnt signaling, promotes colonic cell migration and cancer progression.* Oncogene, 2011. **30**(23): p. 2633-43.

92. Saito-Diaz, K., et al., *The way Wnt works: components and mechanism.* Growth Factors, 2013. **31**(1): p. 1-31.

93. Voronkov, A. and S. Krauss, *Wnt/beta-catenin signaling and small molecule inhibitors.* Curr Pharm Des, 2013. **19**(4): p. 634-64.

94. Abdelhamed, Z.A., et al., *Variable expressivity of ciliopathy neurological phenotypes that encompass Meckel-Gruber syndrome and Joubert syndrome is caused by complex de-regulated ciliogenesis, Shh and Wnt signalling defects.* Hum Mol Genet, 2013. **22**(7): p. 1358-72.

95. Borgal, L., et al., *The ciliary protein nephrocystin-4 translocates the canonical Wnt regulator Jade-1 to the nucleus to negatively regulate beta-catenin signaling.* J Biol Chem, 2012. **287**(30): p. 25370-80.

96. Lancaster, M.A., et al., *Impaired Wnt-beta-catenin signaling disrupts adult renal homeostasis and leads to cystic kidney ciliopathy.* Nat Med, 2009. **15**(9): p. 1046-54.

97. Panjwani, S., et al., *Gardner's Syndrome.* J Clin Imaging Sci, 2011. **1**: p. 65.

98. Easwaran, V., et al., *The ubiquitin-proteasome pathway and serine kinase activity modulate adenomatous polyposis coli protein-mediated regulation of beta-catenin-lymphocyte enhancer-binding factor signaling.* J Biol Chem, 1999. **274**(23): p. 16641-5.

99. Saadi-Kheddouci, S., et al., *Early development of polycystic kidney disease in transgenic mice expressing an activated mutant of the beta-catenin gene.* Oncogene, 2001. **20**(42): p. 5972-81.

100. Mimori-Kiyosue, Y., N. Shiina, and S. Tsukita, *Adenomatous polyposis coli (APC) protein moves along microtubules and concentrates at their growing ends in epithelial cells.* J Cell Biol, 2000. **148**(3): p. 505-18.

101. Dere, R., et al., *beta-Catenin Links von Hippel-Lindau to Aurora Kinase A and Loss of Primary Cilia in Renal Cell Carcinoma.* J Am Soc Nephrol, 2014.

102. Jimbo, T., et al., *Identification of a link between the tumour suppressor APC and the kinesin superfamily.* Nat Cell Biol, 2002. **4**(4): p. 323-7.

103. Kroboth, K., et al., *Lack of adenomatous polyposis coli protein correlates with a decrease in cell migration and overall changes in microtubule stability.* Mol Biol Cell, 2007. **18**(3): p. 910-8.

104. Zumbrunn, J., et al., *Binding of the adenomatous polyposis coli protein to microtubules increases microtubule stability and is regulated by GSK3 beta phosphorylation.* Curr Biol, 2001. **11**(1): p. 44-9.

105. Wheway, G., et al., *Aberrant Wnt signalling and cellular over-proliferation in a novel mouse model of Meckel-Gruber syndrome.* Dev Biol, 2013. **377**(1): p. 55-66.